United States Nuclear Regulatory Commission

Protecting People and the Environment

NUREG/CR-7169

Sensors and Monitoring to Assess Grout and Vault Behavior for Performance Assessment

Office of Nuclear Regulatory Research

AVAILABILITY OF REFERENCE MATERIALS IN NRC PUBLICATIONS

NRC Reference Material

As of November 1999, you may electronically access NUREG-series publications and other NRC records at NRC's Public Electronic Reading Room at http://www.nrc.gov/reading-rm.html. Publicly released records include, to name a few, NUREG-series publications; *Federal Register* notices; applicant, licensee, and vendor documents and correspondence; NRC correspondence and internal memoranda; bulletins and information notices; inspection and investigative reports; licensee event reports; and Commission papers and their attachments.

NRC publications in the NUREG series, NRC regulations, and Title 10, "Energy," in the *Code of Federal Regulations* may also be purchased from one of these two sources.

1. The Superintendent of Documents
   U.S. Government Printing Office
   Mail Stop SSOP
   Washington, DC 20402–0001
   Internet: bookstore.gpo.gov
   Telephone: 202-512-1800
   Fax: 202-512-2250
2. The National Technical Information Service
   Springfield, VA 22161–0002
   www.ntis.gov
   1–800–553–6847 or, locally, 703–605–6000

A single copy of each NRC draft report for comment is available free, to the extent of supply, upon written request as follows:
Address: U.S. Nuclear Regulatory Commission
Office of Administration
Publications Branch
Washington, DC 20555-0001
E-mail: DISTRIBUTION.RESOURCE@NRC.GOV
Facsimile: 301–415–2289

Some publications in the NUREG series that are posted at NRC's Web site address http://www.nrc.gov/reading-rm/doc-collections/nuregs are updated periodically and may differ from the last printed version. Although references to material found on a Web site bear the date the material was accessed, the material available on the date cited may subsequently be removed from the site.

Non-NRC Reference Material

Documents available from public and special technical libraries include all open literature items, such as books, journal articles, transactions, *Federal Register* notices, Federal and State legislation, and congressional reports. Such documents as theses, dissertations, foreign reports and translations, and non-NRC conference proceedings may be purchased from their sponsoring organization.

Copies of industry codes and standards used in a substantive manner in the NRC regulatory process are maintained at—
The NRC Technical Library
Two White Flint North
11545 Rockville Pike
Rockville, MD 20852–2738

These standards are available in the library for reference use by the public. Codes and standards are usually copyrighted and may be purchased from the originating organization or, if they are American National Standards, from—
American National Standards Institute
11 West 42nd Street
New York, NY 10036–8002
www.ansi.org
212–642–4900

Legally binding regulatory requirements are stated only in laws; NRC regulations; licenses, including technical specifications; or orders, not in NUREG-series publications. The views expressed in contractor-prepared publications in this series are not necessarily those of the NRC.

The NUREG series comprises (1) technical and administrative reports and books prepared by the staff (NUREG–XXXX) or agency contractors (NUREG/CR–XXXX), (2) proceedings of conferences (NUREG/CP–XXXX), (3) reports resulting from international agreements (NUREG/IA–XXXX), (4) brochures (NUREG/BR–XXXX), and (5) compilations of legal decisions and orders of the Commission and Atomic and Safety Licensing Boards and of Directors' decisions under Section 2.206 of NRC's regulations (NUREG–0750).

DISCLAIMER: This report was prepared as an account of work sponsored by an agency of the U.S. Government. Neither the U.S. Government nor any agency thereof, nor any employee, makes any warranty, expressed or implied, or assumes any legal liability or responsibility for any third party's use, or the results of such use, of any information, apparatus, product, or process disclosed in this publication, or represents that its use by such third party would not infringe privately owned rights.

United States Nuclear Regulatory Commission

Protecting People and the Environment

NUREG/CR-7169

Sensors and Monitoring to Assess Grout and Vault Behavior for Performance Assessments

Manuscript Completed: July 2013
Date Published: June 2014

Prepared by:
Kenneth A. Snyder[1]
W. Jason Weiss[2]

[1]National Institute of Standards and Technology
Engineering Laboratory
100 Bureau Drive
Gaithersburg, MD 20899-8615

[2]Purdue University
School of Civil Engineering
550 Stadium Mall Drive
West Lafayette, IN 47907-2051

Mark Fuhrmann, NRC Project Manager

NRC Job Code: V-6281

Office of Nuclear Regulatory Research

ABSTRACT

To support performance assessment (PA) of waste vaults and grout monoliths, the National Institute of Standards and Technology (NIST) has performed a preliminary evaluation of the state-of-the-art of sensors, nondestructive evaluation methods, and any relevant geophysical techniques that may be used to quantify changes to the intended chemical (e.g. redox state) and structural properties (e.g. crack initiation, development and propagation) of large engineered waste isolation systems. If the vaults and monoliths remain intact, the system performance should be consistent with the successful performance anticipated from the PA. Events such as cracking, however, could lead to significant changes in the overall vault or monolith performance. Measurement techniques that could be used to detect the onset of cracks and to detect changes in the chemical composition of the matrix are summarized in the context of a monitoring program.

.

TABLE OF CONTENTS

ABSTRACT ..... **iii**

LIST OF FIGURES ..... **vi**

LIST OF TABLES ..... **vii**

EXECUTIVE SUMMARY ..... **ix**

ABBREVIATIONS ..... **xii**

1 INTRODUCTION **1**
1.1 Concrete Grouts and Vaults in Near Surface Waste Disposal Facilities 1
1.2 Performance Assessment 2
1.3 Monitoring 2
1.4 Overview 2

2 REDOX POTENTIAL **5**

3 GROUT OXIDATION **7**

4 CRACKING **9**
4.1 Mechanical Loading of Unreinforced Concrete 10
4.2 Volume Changes Caused by Shrinkage in the Fresh State 12
4.3 Volume Changes Caused by Drying and Autogenous Shrinkage 14
4.4 Volume Change Caused By Temperature Effects 15
4.5 Freezing and Thawing 16
4.6 Corrosion 16
4.7 Alkali-Aggregate Reaction 17
4.8 Cracking in Reinforced Concrete Elements 17
4.9 Sulfate Attack 18
4.10 Summary 19

5 MODELING SERVICE LIFE **21**

6 CHEMICAL STATE SENSORS & NDT METHODS **23**
6.1 Moisture/Water Content 23
6.2 pH 24
6.3 Redox Potential 26
6.4 Radionuclide Detection 27

7 STRUCTURAL HEALTH MONITORING **29**

8 STRUCTURAL HEALTH MONITORING TECHNIQUES **31**
8.1 Acoustic Emission 31
8.2 Electrical Properties of the Concrete 32
8.3 Electrical Properties of Films or Surface Coatings 33
8.4 Magnetic Crack Opening Sensors 35
8.5 Visual Imaging, Thermal Imaging, and Shearography 36
8.6 Ultrasonics 36
8.7 Geophysics 37
8.8 Example Application: Pipeline Subjected to Ground Motion 37

9 POTENTIAL STRUCTURAL HEALTH MONITORING SOLUTIONS **39**
9.1 Monitoring the Vault 39
9.2 Monitoring the Grout 40

10 CONCLUSION **41**

11 REFERENCES **43**

LIST OF FIGURES

Figure 1- Types of cracking observed in concrete elements. AAR: Alkali-Aggregate Reaction. ASR: Alkali-Silica Reaction. DEF: Delayed Ettringite Formation. (From TRB 2006) 9

Figure 2- Stress-strain response of aggregate, concrete, and cement paste (after Mindess et al. 2002)..... 10

Figure 3- Composite model for concrete mechanical response characterized by the stress (σ) strain (ε) response of the material (After Jansen and Shah 1997). 12

Figure 4- An example of differential settlement over the surface of the reinforcing bar (after Kwak et al. 2010). 13

Figure 5- (a) Stress development and (b) conceptual description of relaxation (after Weiss 1999)..... 15

Figure 6- Relationship between stiffness degradation (E/E_O with 1.0 being undamaged) and the degree of saturation for non-air entrained (circles) and air entrained concrete (squares) (after Li et al. 2012). 16

Figure 7- An illustration of the role of cracking perpendicular to reinforcing steel and the accompanying debonding that occurs along the reinforcing bar: a) Illustrated conceptually (after Goto 1971) and b) Measured experimentally using image correlation (after Pease et al. 2010)..... 18

Figure 8- An illustration of a through crack in a reinforced concrete element (after Bernard and Brühwiler 2003). 18

Figure 9- A schematic of a combination pH electrode (adapted from Ritz and Collins 2008)..... 25

Figure 10- A schematic of how crack formation can influence transport processes in concrete: a) environmental causes of cracking, b) distributed (micro-cracks) and coalesced cracks, and c) pathways for both ingress and egress of moisture, gases, and dissolved species. 29

Figure 11- Acoustic activity: a) the spatial distribution of activity during loading in freeze-thaw damaged samples, and b) the size of the damage zone when measured under tensile loading as freeze-thaw damage increases (E/E_o decreases) (after Yang et al. 2006). 32

Figure 12- Electrical response of cracked concrete: a) an illustration of the sample geometry used for electrical measurements and b) the measured electrical response as a function of crack orientation..... 33

Figure 13- A conceptual illustration of acoustic emission sensors and conductive surface coatings on restrained slab elements..... 34

Figure 14- A typical picture of a cracked slab at the mid-span (at the notch location). The four strips of conductive surface coating and their electrical connections are also shown. 34

Figure 15- Time of cracking detected by monitoring the strain in steel ring and resistance increase of copper tape applied to the surface of mortar in restrained ring test (Pour Ghaz et al. 2011). 35

Figure 16- Illustration of a magnetic crack opening sensor (after Pour-Ghaz et al. 2011)..... 36

Figure 17- A schematic of how conductivity strips or acoustic sensors could be placed in an array on the surface of a saltstone monolith (or interior wall of the vault) or on the exterior surface of the concrete vault to help monitor the overall performance of the system. 39

Figure 18- Schematic of a single-pole approach to installing sensors in a grout monolith during construction. A similar configuration using two or more rods, could also contain electrodes for resistivity measurements. 40

LIST OF TABLES

Table 1- Oxidation states for a few of the elements that may play a role in the redox potential of the saltstone waste form pore solution. 5

Table 2- pH electrodes recommended for water having elevated concentrations of sodium and other monovalent major cations and sulfides (Ritz and Collins 2008) 26

EXECUTIVE SUMMARY

To support performance assessment (PA) of waste vaults and grout monoliths, the National Institute of Standards and Technology (NIST) has performed a preliminary evaluation of the state-of-the-art of sensors, nondestructive evaluation methods, and any relevant geophysical techniques that may be used to quantify changes to the intended chemical (e.g. redox state) and structural properties (e.g. crack initiation, development and propagation) of large engineered waste isolation systems. Specifically, if the vaults and monoliths remain intact, the system performance should be consistent with the successful performance anticipated from the PA. Events such as cracking, however, could lead to significant changes in the overall vault or monolith performance. Ideally, sensors could be used to not only detect the occurrence of these events, but also give an indication of the impact these events have on the vault or monolith system performance.

Based on the preliminary evaluation, techniques and/or combinations of techniques and sensors have been identified that may be amenable to obtaining quantitative data for evaluating and modeling performance of the vault or of the grout that are important to waste sequestration such as redox state, porosity and crack development. This information could be used to assess the need for future research projects to develop or deploy sensors and other approaches for monitoring these materials. This could be accomplished by further improvements of the techniques in future studies.

The nondestructive evaluation (NDE) methods and sensor technologies for concrete structures have been discussed in the context of data to compare with service life prediction. The present paradigm of nondestructive testing (NDT) is to determine the current state of a structure. Although this approach has broad application, such as for evaluating the structural integrity of a concrete structure after a catastrophic event such as an earthquake, present techniques have limited utility in estimating long-term performance, especially as it relates to serviceability states such as fluid or contaminant transport.

To facilitate such PAs, the report contains an assessment of existing NDT methods and sensor technologies, discussed in the context of collecting information relevant to service life prediction (SLP) tools. The conceptual models typically employed by SLP tools illuminate the physical and chemical parameters that have relevance to the analysis. Those NDT methods and sensor technologies that give direct, or indirect, estimates of these parameters are discussed. A combination of resident expert assistance, a review of technical and commercial literature, discussions with external practitioners, and on-site field inspection were used to ascertain the broadest perspective of available techniques that may contribute to performance assessment of grouts and vaults. Critical service life model parameters and the tests required to quantify the relevant property, were identified along with some measure of the required accuracy and precision of these tests. Upon identifying technology gaps (a lack of technology development or a lack of standardized test method), a strategy was drafted for meeting these needs.

ABBREVIATIONS

AAR	Alkali-Aggregate Reaction
ACR	Alkali-Carbonate Reaction
ASR	Alkali-Silica Reaction
CMH	Chilled Mirror Hygrometer
DEF	Delayed Ettringite Formation
DOE	U.S. Department of Energy
HLW	High-Level Waste
NDAA	National Defense Authorization Act
NDE	Nondestructive Evaluation
NDT	Nondestructive Testing
NIST	National Institute of Standards and Technology
NRC	U.S. Nuclear Regulatory Commission
NSWD	Near Surface Waste Disposal
PA	Performance Assessment
SLP	Service Life Prediction
SRS	Savannah River Site
WIR	Wastes Incidental to Reprocessing

1 INTRODUCTION

U.S. Nuclear Regulatory Commission (NRC) has both consultation and monitoring roles for certain Department of Energy (DOE) waste resulting from reprocessing of spent nuclear fuel as required by the Ronald W. Reagan National Defense Authorization Act (NDAA) of 2005. These "Wastes Incidental to Reprocessing" (WIR) are contained in cementitious monoliths that in turn are contained within waste vaults and subsurface tanks. The criteria against which DOE Performance Assessments are evaluated are given in 10 CFR 61.40-44. To accomplish its objective, NRC uses data and models to understand and predict the properties of large grout based waste isolation structures so that changes in behavior over long-times can be anticipated and the long-term performance can be evaluated. The critical performance characteristics can only be estimated, and their behavior over long time periods is uncertain. Quantifying the properties of these materials is important because, from them, the release of radionuclides is estimated and doses calculated.

These uncertainties regarding the long-term performance of cementitious materials for large concrete structures have highlighted the need for monitoring methods to evaluate the properties of cementitious grouts that have an impact on long-term safety. Moreover, there are questions about changes in cementitious waste materials, such as saltstone and high-level waste (HLW) tank backfill grouts, that could lead to crack formation, oxidizing conditions, and moisture transport that could result in contaminant transport from these systems. In particular, water and oxygen transport through these materials could result in unacceptable peak doses, so it will be important to better quantify the long-term changes that can take place, along with the chemical changes within the grout. Because sufficiently sophisticated transport and reaction models do not yet exist to predict these changes, the more practical approach is a thorough monitoring program that combines measurement, (less sophisticated) modeling, and remediation planning. This report will address the measurement methods that can contribute, in a meaningful way, to such a monitoring program.

There are three broad classes of nondestructive evaluation (NDE) technologies to consider for a comprehensive monitoring program: chemical, electrical, and mechanical sensors. The chemical state sensors have been used in geochemical analysis, the electrical sensors have been used in the detection and measurement fields, and the mechanical sensors have been used in the civil engineering field. Moreover, each type of sensor only provides a limited and incomplete picture of the state of the entire system. Although laboratory tests exist for determining the chemical/mineralogical state of a cementitious system, the comprehensiveness of these tests for ascertaining critical chemical information like redox potential is unlikely.

In addition, the chemical environment of a cementitious vault or saltstone waste form is different from a geological environment. The pore solution of a cementitious material is alkaline (Taylor 1990), with a pH typically greater than 12. Saltstone waste forms are a mixture of blended cementitious materials and a concentrated solution (28 % solids by mass) containing sodium hydroxide, sodium nitrate, and sodium nitrite (Dixon et al. 2008). Although the hydrated phases have some similarity with geological minerals, the applicability of geochemical tests to cementitious systems is uncertain. Fortunately, many of the mineral and chemical characteristics of rocks, soils, and cementitious materials are very similar.

1.1 Concrete Grouts and Vaults in Near Surface Waste Disposal Facilities

The components of the near surface waste disposal (NSWD) facilities infrastructure that are being considered are the engineered cementitious elements designed as physical and/or chemical barriers to radionuclide transport through waste vault and grout monoliths. These cementitious materials are typically a grout formulation composed of a cementitious binder (a powder), fine aggregate, and "mix water". The mix water could either be a natural or municipal water supply (waste vault), or it could be a liquid wastes incidental to reprocessing (WIR) to be immobilized within the cementitious matrix (grout monolith). The saltstone contains very little portland cement, but a large quantity of waste solution. Both saltstone and tank backfill grouts are made to be very fluid so they are self-leveling.

These cementitious elements typically have attributes that can make it difficult to develop reliable NDE and sensor strategies:

Inaccessibility: The cementitious elements are typically contained within another (concrete or steel) structure that may be partially or completely buried underground, with limited accessibility to waste. An externally applied testing strategy would have to penetrate the outer engineered barriers. Alternatively, sensors and testing apparatus buried with the waste may have to perform many decades (or centuries) without replacement.

Extreme Service Life Requirements: The half-lives of the radionuclides immobilized in these cementitious matrices will require that the engineered barrier render them inaccessible for hundreds or thousands of years. Therefore, these structures need assured performance that is far longer than any existing engineered cementitious structure. Moreover, near surface disposal facilities are subject to the effects of weathering, moisture, oxidation, etc.

1.2 Performance Assessment

An important aspect of conducting a performance assessment (PA) is estimating the probability that a facility will continue to perform its intended purpose throughout the licensing period. If the internal and external conditions at a facility never change, one would merely need to perform a condition assessment of the built facility to ascertain whether the facility would be acceptable. The uncertainty in the possible changes that may occur, however, make a PA difficult to perform. Moreover, even if one can predict what future changes may occur, one still needs to have a way of understanding how these changes will impact future performance.

Predicting these effects on future performance can be very challenging. These systems differ somewhat from typical industrial applications of cementitious matrices. In general, existing performance prediction models for cementitious materials are based on mixtures where the binder materials are at least 50 % (by mass) portland cement. In addition, the standardized tests for durability were developed based on the assumption that the binding phase would be mostly portland cement mixed with water. Moreover, few, if any, of the performance prediction models have been validated for mixtures made with high concentrations of sodium hydroxide, sodium nitrate, and sodium nitrite, which are primary components of saltstone (Dixon 2008).

1.3 Monitoring

Monitoring may be an effective means of supplementing service life prediction tools through inspections and assessments (Naus and Graves 2000, Naus 2009). Borrowing from the strategy used for nuclear power plants, there may be value in moving away from preventative (time based) maintenance strategy to a component condition based strategy (IAEA 2007). A condition based monitoring strategy requires an integration of diagnostic and performance data, both present and historical. The diagnostic data may consist of periodically going to the facility with test equipment and performing measurements, or it may consist of permanent sensors embedded in, or attached to, the waste vault or the grout monolith. Through monitoring, one can detect gradual changes in properties (e.g., leaching), or dramatic discrete changes (e.g., cracking). Monitoring has the advantage that it can provide constant feedback, and can be coupled to on-going service life model calculations.

Effective long-term monitoring is complicated by the extreme performance requirements of the sensors that are shared by monitoring strategies for geological repositories (IAEA 2001). The sensors may be permanently implanted into the structure, have a specific period of use (such as for the detection of early age cracking), or they may be designed for periodic replacement. The decision could be based, in part, on the integrity of the resulting “penetration,” as the inclusion of sensors cannot compromise the vault performance. If the integrity of the penetration is critical, replaceable sensors may not be an effective option. In such cases, the sensor would have to remain effective for the duration of the expected monitoring program, or would have to rely upon excessive redundancy. Alternatively, remote non-intrusive survey condition assessment measurement techniques may be the most favorable.

1.4 Overview

The following sections cover a number of important topics to be considered when evaluating strategies for isolating radionuclide waste in cementitious grouts or vaults:

***Reduction/Oxidation Potential*:** One of the critical material parameters controlling the overall performance of the engineered structure is the reduction/oxidation (redox) potential within the pore solution. The section highlights the role that oxidation plays in controlling the redox potential of a system.

***Grout Oxidation*:** Different mechanisms by which the cementitious system could oxidize, and thus develop an undesirable redox potential, are discussed. Different oxygen pathways, including both liquid and gas infiltration, are discussed, particularly in the context of cracking.

***Cracking*:** Cracks can significantly increase the rate of gas and liquid transport into a structure.

***Modeling Service Life*:** Because these systems must perform satisfactorily for hundreds or thousands of years, there are no existing engineered barriers with which to compare. Instead, the future performance of the system can only be surmised by estimating the expected performance through the use of service life models.

***Chemical & Physical Sensors*:** Because no service life prediction model for a cementitious system has ever been validated over the very long time periods of performance required here, the more reliable approach is to couple service life modeling to a monitoring strategy. Available chemical and physical sensors are discussed in the context of supporting service life models.

2 REDOX POTENTIAL

One of the critical factors influencing the overall performance of the radioactive waste disposal systems being considered is the reduction-oxidation (redox) potential of the aqueous solution filling the pores of the cementitious waste form. This "pore solution" is in equilibrium with the hardened mineral phases present, and the scenario is analogous to a groundwater in equilibrium with the soil and geology.

The redox potential characterizes the chemical state of a solution when a chemical element is present in two different oxidation states: e.g., Fe^{+2} and Fe^{+3}. Some of the elements commonly found in saltstone waste forms, and having multiple oxidation states, are given in Table 1 below. Oxidation leads to an increase in the oxidation state, and reduction leads to a decrease in the oxidation state. Oxidation is often accompanied by the release of a proton that lowers the pH, and reduction is often accompanied by the consumption of a proton that increases the pH.

Table 1-Oxidation states for a few of the elements that may play a role in the redox potential of the saltstone waste form pore solution.

Element	Symbol	Oxidation States
Sulfur	S	6+, 4+, 0, 1-, 2-
Nitrogen	N	5+, 3+, 0, 3-
Iron	Fe	3+, 2+
Manganese	Mn	2+, 3+, 4+, 6+, 7+

The oxidation-reduction reaction for a redox pair can be expressed as follows (Langmuir 1997):

$$\underset{\text{oxidized}}{aA + bB + ne^-} = \underset{\text{reduced}}{cC + dD} \tag{1}$$

If the species appearing on each side of the reaction in Eqn. 1 are in two separate containers that are connected by a salt bridge, there would be an observable electrical potential between the two containers. This *redox potential* can be estimated from the activity of the relevant species:

$$E_h = E^o - \frac{RT}{nF}\ln\left(\frac{\{C\}^c\{D\}^d}{\{A\}^a\{B\}^b}\right) - \frac{mRT}{nF}\ln\{H^+\} \tag{2}$$

The quantity *R* is the universal gas constant, *T* is the absolute temperature, *F* is the Faraday constant, *n* is the number of electrons exchanged, and *m* is the number of protons exchanged. The quantity E^o is the standard potential for the half-reaction, and is related to the change in the Gibbs free energy for the reaction (ΔG_r^o):

$$E^o = \frac{-\Delta G_r^o}{nF} \tag{3}$$

Often, the redox potential is expressed as the pE, to represent (by analogy to pH) the negative common logarithm of the electron activity: $\mathrm{pE} = -\log_{10}\{e^-\}$. The pE is related to the redox potential through the following relationship (Stumm and Morgan 1981):

$$\mathrm{pE} = \frac{F}{(\ln 10)RT}E_h \tag{4}$$

In nature, redox reactions occur rather slowly, and the systems are not in equilibrium. The reaction is often limited by the type of mineral phase each species is associated with, the gain in free energy from the redox reaction, the availability of adequate catalysts, and the availability of oxygen (Schüring et al. 1999). Generally, the mineral phases involved are comparatively stable. Although the redox potential depends, in part, on the rate of reaction, the value is most strongly influenced by the quantity of

reductant that is present. As oxidation occurs, the redox potential changes relatively little until all the reductant is consumed. After which, the redox potential will increase dramatically.

Blast furnace slag contains sulfides, a reduced form of sulfur, which is beneficial for immobilizing certain radionuclide wastes. Angus and Glasser (1986) demonstrated that the addition of about 4.5×10^{-4} moles of Na_2S per gram of portland cement produced a cement paste having a pore water (solution) with a redox potential (E_h) approximately equal to that of a grout paste prepared with blast furnace slag. The use of blast furnace slag for immobilizing technetium in a grout has been studied for more than twenty years (see, for example, Gilliam et al. 1988). The relative E_h values for the slag systems were approximately -250 mV, compared with approximately +400 mV for the fly ash and portland cement samples. As for its practical effectiveness, the addition of ground blast furnace slag to grout has been shown to reduce the leaching of technetium by several orders of magnitude (Gilliam et al. 1990).

The effectiveness of the sulfide, however, has only been studied in the context of the initial state of the system. Relatively little data exist on the long-term effectiveness of sulfides in cementitious matrices, particularly near surface elements exposed to weather and to groundwater.

3 GROUT OXIDATION

Grout oxidation contributes directly to the redox potential, and therefore, the vault performance. In an air tight and water tight vault, the waste form would consume the available oxygen that is present, after which the redox potential would remain stable. In reality, however, the waste form will likely be cast into a concrete vault that is neither air-tight nor water-tight. Therefore, the overall performance of the facility will depend upon the degree to which the concrete vault limits the passage of oxygen and groundwater.

As the transport of oxygen (diffusing through the pore solution) or the flow of groundwater (containing dissolved oxygen) through the concrete vault is nearly inevitable, the duration over which the facility performs as intended will depend upon the rate of oxygen ingress and the quantity of reductant that is initially present. Upon passage of oxygen, and subsequent oxidation, the redox potential will increase, albeit slowly. When the sulfur in the slag has been oxidized to sulfate, the redox potential will increase in a step-wise manner to the redox potential controlled by the next dominant redox pair: e.g., iron(II/III), manganese(IV/II). The oxidation will continue, with ensuing step-wise increases, until all redox pairs have been oxidized, and the grout reaches equilibrium with the exterior ground water (Kaplan 2003). Systems that have oxidized to this state typically have a redox potential in the mV range.

The rate that oxygen penetrates the vault and comes into contact with the waste form depends on the properties and condition of the exterior concrete vault, and the vault's environment. Generally, there will be a very large earthen cover to shed water away from the vault. This earthen cover can reduce the rate of oxygen or fluid transport and sensors can be placed throughout this layer. If the concrete vault remains intact, and the vault is located in an arid environment, the vault pore water will slowly evaporate, creating air-filled pores that increase the rate of oxygen (gas) diffusion through the vault. If the intact vault is in a humid environment, but above the water table, oxygen diffusion through the water-filled vault pores will be dramatically lower than in the arid environment. If the vault is below the water table, oxygen will be carried by groundwater ingress, the rate of which would be controlled by the concrete hydraulic conductivity. If cracks form in the concrete vault, the rates of the aforementioned oxygen transport scenarios are magnified accordingly.

Once oxygen has penetrated the vault and has come into contact with the waste form, the kinetics of the waste form oxidation are controlled by the rate of oxygen transport through the waste form. If the waste form remains intact, oxygen must either diffuse through the waste form pore solution or migrate through the grout matrix by advection. If the waste form were to crack, however, these cracks would provide direct pathways for oxygen to penetrate the interior of the waste form. Moreover, the cracks not only accelerate the rate of oxidation, they also serve as pathways for the release of radionuclides after the waste form has oxidized sufficiently.

Interestingly, the degree of saturation of the porosity by water is an important factor affecting groundwater infiltration, oxygen diffusion, and cracking. Water permeation and oxygen diffusion occur primarily through the pores within the hardened cement paste fraction of the matrix. Permeation will occur through the liquid-filled pore space, and permeation occurring continually over a very long time will eventually saturate the system. By contrast, oxygen diffusion occurs through both the gas-filled and the water-filled pore space; oxygen diffuses through the gas phase, and is dissolved into the liquid phase, where it then diffuses at a much slower rate. As a result, the rate of oxygen diffusion through a saturated specimen is extremely low, while oxygen diffusion through a dry sample is far greater, and diffusion through a partially-saturated system is somewhere in between (Page and Lambert 1987). Therefore, the rate of transport through either the vault or the saltstone will depend strongly on the degree of saturation of the paste.

Furthermore, if drying (either self-desiccation or external drying) occurs in the vault or the saltstone grout, the shrinkage stresses can lead to cracking. If the vault dries from the outside, the outside layer will be in tension, giving rise to cracks, which further accelerates the rate of oxygen diffusion.

One approach to a monitoring strategy for waste form grouts could be to detect events that would hasten the rate of oxidation. Specifically, an approach could include instrumentation for detecting three phenomena:

- Groundwater infiltration

- Changes in moisture content (vault and saltstone grout)
- Crack initiation and propagation (vault and saltstone grout)

The advantage to such an approach is that it does not rely upon chemical sensors, which have not yet been demonstrated for very long-term reliable service (without cleaning or replacement). Furthermore, detecting moisture and cracks can be done using techniques involving embedded sensors, for which there may exist relatively long-term performance data (e.g., decades)

4 CRACKING

One of the most significant contributors to oxidation and any subsequent release of radionuclides will be cracking, both in the vault structure and in the saltstone monolith. Although there is general awareness that cracking can be caused by unanticipated mechanical loading, it should be noted that cracking can also be caused by environmental conditions. The cause of the cracking is important as it may have profound implications on the crack morphology, which can greatly influence the relative contribution to transport and the subsequent impact on overall performance. Because there are many factors influencing cracking, and its consequences, a brief review of these types of cracks is provided.

The onset of cracking can be roughly divided into two categories: distress at early age (before hardening), and distress at later age (after hardening). Further classification is shown schematically in Figure 1 (after Weiss et al. 2000). Cracks that form at early ages and in low strength materials typically go around the aggregate, while cracks that occur at later ages, or in higher strength materials, can either go around the aggregate or through the aggregate, fracturing the aggregate itself.

While not a complete listing of all the causes for cracking, Figure 1 illustrates that numerous causes for cracking exist. While the following discussion provides a brief overview of the causes for cracking, a more exhaustive discussion can be found elsewhere in the literature (ACI 1990, TRB 2006).

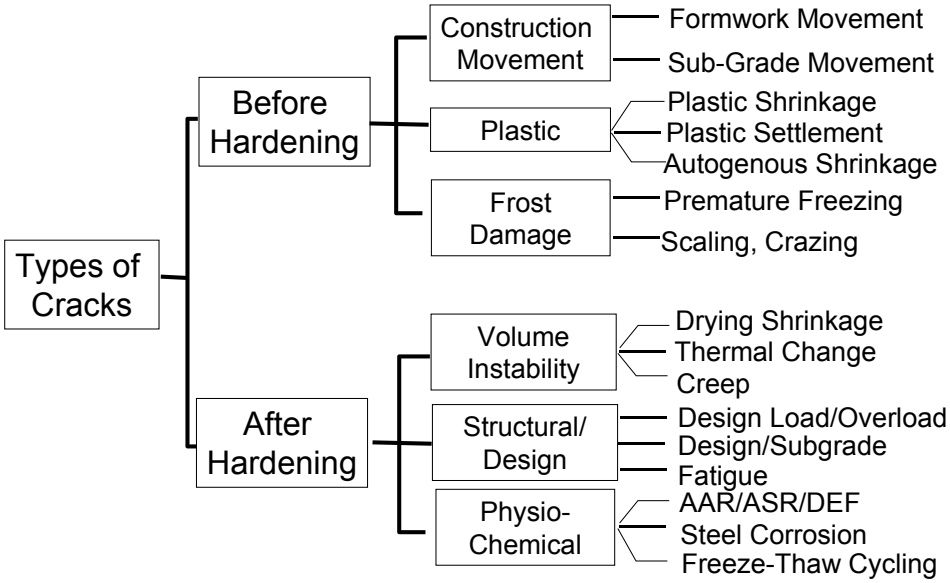

Figure 1- Types of cracking observed in concrete elements. AAR: Alkali-Aggregate Reaction. ASR: Alkali-Silica Reaction. DEF: Delayed Ettringite Formation. (From TRB 2006)

Cracks that occur during or shortly after construction are generally referred to as plastic shrinkage, settlement, or construction movement related cracks. Cracks can also develop at relatively early ages due to the restraint of thermal and hygral shrinkage movements (i.e., volume change due to capillary and disjoining pressure, Wittmann 2009). Cracking can develop in the concrete at later ages due to freezing and thawing, sulfate attack, alkali silica reaction, and reinforcing steel corrosion. The freezing and thawing, alkali aggregate reaction, and corrosion induced cracking occurs as a result of an internal expansion that is primarily caused by chemical attack of the reinforcing steel, aggregate, or by the freezing pore water.

It is the premise of this work that cracks can act as conduits that accelerate the ingress of liquids or gases. Although numerous factors influence whether a concrete would be expected to crack due to environmental effects, it can be simply stated that cracking will occur if the stress that develops in response to internal expansion or restraint of a volumetric contraction results in stress that exceeds the strength (or fracture resistance) of the material. The following section describes the main types of cracking that may occur.

4.1 Mechanical Loading of Unreinforced Concrete

Concrete, by comparison with pastes (saltstone) or mortars (tank backfills), is a composite material that is made of aggregates held together by a hardened cementitious paste. While the independent response of a cement paste and the aggregate to an applied load is nearly linear over a broad range of stress, as shown in Figure 2, it can be seen that response of the composite concrete is relatively non-linear. This non-linearity can be attributed to the development of small cracks (microcracks) throughout the concrete matrix as load is applied (Hsu et al. 1963). While this is a primary reason for the non-linearity and is generally confirmed with microscopy or acoustic emission measurements, others have suggested that this may be attributed to existence of a weak bond or interfacial transition zone between the aggregate and the paste matrix. While these cracks occur over a wide range of load levels they can be attributed to the development of high local stresses that occur at the interface of the aggregates and paste (Shah and Slate 1965). These cracks are typically not wide enough to influence transport substantially (see, for example, Pabalan et al. 2009).

Even in the absence of mechanical loading, concrete is thought to develop some micro-cracking due to differential stiffness and movement between the matrix and aggregate (Shah and Slate 1965). It is frequently assumed however that the amount of microcracking that develops at low load levels (less than 30 % of the peak load) is relatively small. This is confirmed with acoustic emission measurements that record very few acoustic events at low load levels (Puri and Weiss 2006). It is expected that the stresses within the grout are designed to remain below the peak load (i.e., the tensile strength or compressive strength of the material). The grouts inside the tanks or vaults will likely experience very low levels of mechanical loading other than self weight or loading induced by cracking that may occur within the vault.

Pabalan et al. (2009) suggested that discrete interface cracking (i.e., the cracks that occur at no load or very low load levels) should likely not be considered explicitly in models since these cracks likely exist in the laboratory samples that transport has been measured on. As a result these cracks are likely already included in the laboratory measurements of these properties. While this may be true, and it is an interesting observation, it points out the importance of comparing the crack behavior among lab samples, field samples, and models to ensure that lab samples and models incorporate the most important features of cracks found in field specimens.

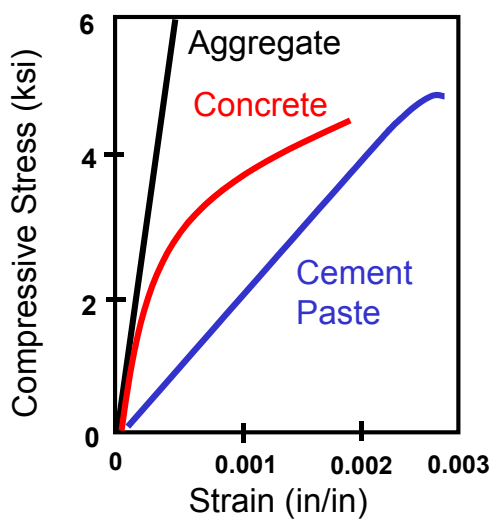

Figure 2- Stress-strain response of aggregate, concrete, and cement paste (after Mindess et al. 2002).

After the load level reaches approximately 30 % to 50 % of the peak load, microcracking increases resulting in a slight decrease of the stiffness of the concrete. This increase in microcracking is consistent with increased acoustic emission activity (Puri and Weiss 2006). The cracks that occur

during this period generally occur at the interface of the matrix and aggregate. While this may be attributed in part to an interfacial transition zone with different properties of the matrix it can also be attributed to the high level of restraint caused by the aggregate and the differences in elastic properties between the aggregate and matrix. The microcracks that occur up to approximately 50 % of the peak load tend to be relatively small and are disconnected cracks in the material. As a result it is generally believed that these microcracks tend to have a small impact on transport in most materials.

As the loads level approaches 75 % to 85 % of the peak, the slope of the load-displacement curve begins to show a greater deviation from linearity as the cracks begin to coalesce and localize in one region of the specimen. This cracking can be observed upon inspection under the microscope and acoustic emission measurements also show an increase in activity when the load reaches this level. The coalesced crack will eventually become a visible crack at or after the peak load is reached.

Depending on how the specimen is loaded (i.e., load control, displacement control) the crack may result in sudden failure (load control) or it may continue to develop and grow after the peak load is reached (displacement control) resulting in large visible cracking. After the peak load is achieved the specimen begins to demonstrate strain softening behavior resulting in a gradual decrease in load carrying capacity with increasing strain. In reinforced concrete elements, the width of the crack opening will be controlled by the diameter and the amount of the reinforcing steel.

Although the stress-strain response of concrete is often used to estimate the Young's modulus of the material, which suggests that the stress-strain response is an intrinsic material property, the stress (σ) strain (ε) response does, in fact, depend on the size of the specimen used in the testing. Under uniaxial compression, prior to achieving the peak stress, the specimen exhibits relatively little hysteresis, consistent with distributed (non-overlapping) cracks occurring throughout the specimen. In this region of the curve, it is generally assumed that damage is well distributed throughout the material. In the post-peak region of the stress-strain curve, however, the response of concrete can be idealized as two types of materials, the bulk concrete and the damage zone, which behave quite differently from each other (Bazant 1976, Hillerborg et al. 1976). It is in this region that the size dependence and localization become important. To illustrate this, a typical model for unloading of these parts has been shown in the lower stress-strain curve in Figure 3. The bulk region of the sample is generally considered to act as an elastic material or a material that demonstrates some damage due to microcracking but it is linear on unloading. A damage index may make sense in this region (note the damage index (D) is typically related to the degradation in elastic modulus (E) as compared to the original elastic modulus (E_O) as $D = 1-E/E_O$). The damaged zone can be characterized with a pre-peak behavior that may be like that in the bulk region. However, after the peak is reached the material generally has a stress crack opening type of response. This is important since it illustrates the importance of separating the localized region of cracking from the bulk behavior. This also has implications on transport which will be discussed later in this document as transport in the bulk region can be quite different than transport that occurs in the damage zone or localized crack. As such it may be convenient to split material behavior into these two regions.

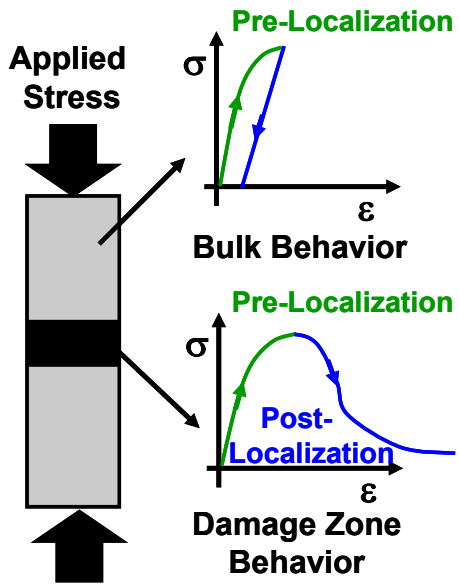

Figure 3- Composite model for concrete mechanical response characterized by the stress (σ) strain (ε) response of the material (After Jansen and Shah 1997).

While the previous section has illustrated the compressive response, the same ideas can be extended to tensile loading. While the size of the localized region in compression is typically related to the diameter of the specimen (Jansen and Shah 1997; Puri and Weiss 2003), it is smaller for specimens loaded in tension or flexure and is approximated as 2 or 3 times the size of the largest aggregate used in the concrete (Bazant and Planas 1998 and Yang et al. 2006). In specimens loaded in tension or flexure the damage zone is where the visible crack will appear.

The location of cracking in a structure typically develops where there is a combination of the highest stress and the weakest plane. This can occur when there is a reduction in concrete section, a preexisting flaw, or an area of stress concentration. The study of the development of how cracks develop and propagate in a structure is commonly referred to as fracture mechanics. Over the last four decades significant research has been performed to better understand the fracture processes in concrete. Fracture mechanics differs from continuum mechanics approaches in that it relates local stress levels (stress intensity) to the existence of a crack, and to the energy required to propagate that crack. Developments in non-linear fracture mechanics research over the last four decades have shown that concrete is a quasi-brittle material which exhibits pre-critical (i.e. pre-peak) crack growth (fracture process zone) and strain softening (post-peak stress transfer). Although the subject of fracture mechanics is beyond the scope of this document, there are several recent books that summarize the main attributes of concrete fracture (Shah et al. 1995; Bazant and Planas 1998; Van Mier 1999).

The process of cyclic mechanical loading can also cause crack initiation and evolution in plain concrete, resulting in the observed progressive deterioration of the mechanical properties, such as strength. One hypothesis attributes progressive deterioration to failure at the bond between the coarse aggregate and the matrix. Another hypothesis attributes the fatigue failure in concrete to the coalescence of pre-existing micro-cracks in the matrix, resulting in a single localized macro-crack. For this report a distinction will not be made for cracks made by static or fatigue loading. For further information on fatigue behavior of plain and reinforced concrete the reader is referred to the ACI 215R-74 committee report titled “Consideration for Design of Concrete Structures Subjected to Fatigue Loading” (ACI 1997).

4.2 Volume Changes Caused by Shrinkage in the Fresh State

Cracks that develop during or shortly after construction include cracks due to plastic shrinkage, settlement, or construction movements. Plastic shrinkage is generally thought of as being due to capillary stress caused by the rapid evaporation of water from freshly placed concrete (ACI 2007). It is

generally assumed that when the bleed rate exceeds the rate of evaporation the concrete will be safe from plastic shrinkage cracking as a protective layer of water will be present on the surface of the concrete. It is assumed that this would be the case for grouts, for example. If the evaporation rate is higher than the bleed rate, capillary stresses can develop in the material that could lead to cracking (Lura et al. 2007). It is also important to recognize that there are two other sources of volume change that can occur during this time period that may lead to cracking. First, differential settlement can be important for any concrete/saltstone that is cast with a difference in cross section or with reinforcing steel. The concrete 'settles' in a fresh state as the cement and aggregates are denser than water. As the cement and aggregate settle faster water is left behind 'appearing as bleed water' on the surface. When the section is all the same thickness and there are inclusions that the material is cast around (e.g., inclusions could include reinforcement, or blockouts, or forms for a change in section height), the material will experience differential settlement above the inclusion and next to the inclusion leading to the development of stress in the freshly placed material that can ultimately lead to cracking (Qi et al. 2003, and Kwak et al. 2010). This is illustrated in Figure 4, showing data from Kwak et al. (2010), where the y-axis illustrates the settlement at the surface of the concrete shortly after concrete placement and

the x-axis measures the horizontal distance from the reinforcing bar. While this is shown with respect to differential settlement occurring over a reinforcing bar, it also commonly occurs over pipes or changes in section depth and as such it may be specifically related to potential settlement around embedded pipes in tanks.

The second type of volume change that can lead to cracking is autogenous shrinkage that occurs in response to chemical shrinkage. While this occurs in all materials, it is important to note that the magnitude of shrinkage increases substantially as the water to cement ratio decreases. It is mentioned here since this shrinkage begins to occur as the water comes in contact with the cement (Sant et al. 2006). It should also be noted that during this time the assumption of shrinkage being isotropic is violated and the shrinkage occurs preferentially in the vertical direction.

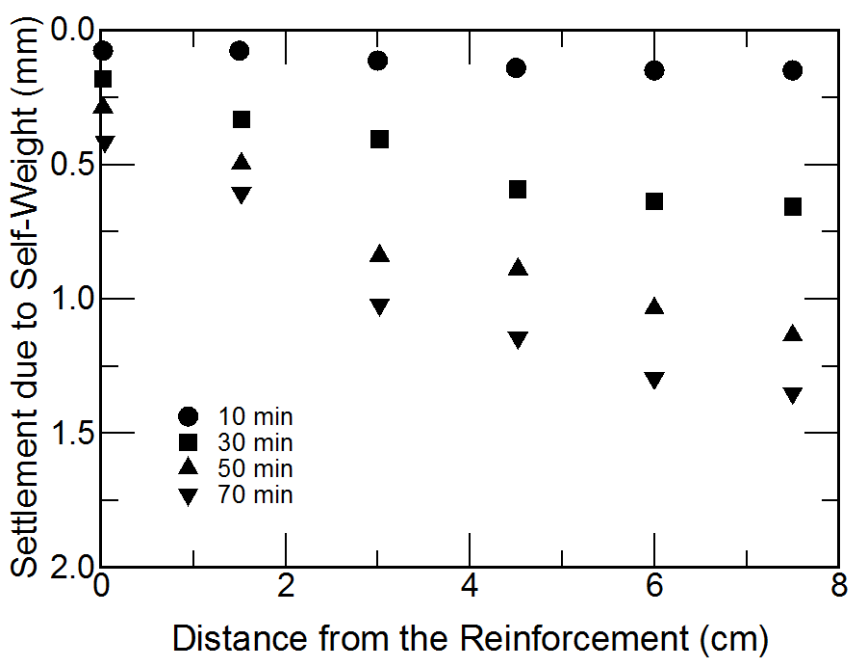

Figure 4- An example of differential settlement over the surface of the reinforcing bar (after Kwak et al. 2010).

It is expected that specifications can be developed to substantially reduce this plastic cracking in vault structures of the type being built at Savannah River Site (SRS) and as such this report will not address them in detail. There are relevant test methods such as the standardized plastic shrinkage cracking test

ASTM C1579 (ASTM 2013) and the standardized autogenous shrinkage test ASTM C1698 (ASTM 2009b). Strictly speaking, these cracks would become evident during the first day or two after construction or immediately after the formwork is removed.

It should be noted that early age volume changes may be important for the saltstone materials that are being placed inside the vault; however more information would be needed about the early age volume changes expected for those materials. For example, the saltstone material could shrink and pull away from the wall resulting in a 'gap' between the wall of the containment and the outer surface of the salt stone. This, if the volume change is sufficient, could facilitate transport (gas or vapor) along the outer edge of the saltstone. Also, if the saltstone were restrained during casting it may itself crack into smaller blocks that could increase the diffusion of gas (oxygen) into the saltstone. This could alter the diffusion distances assumed in modeling for example. To better answer this question a more detailed analysis would be needed for the shrinkage and mechanical properties of the materials at early ages following a protocol like ASTM C1581 (ASTM 2009a) or ASTM C1698 (ASTM 2009b) for example.

4.3 Volume Changes Caused by Drying and Autogenous Shrinkage

There are two types of shrinkage (volume change) that can occur in hardened concrete due to water related (hygral) effects. These two types of shrinkage are generally referred to as autogenous shrinkage and drying shrinkage. Drying shrinkage occurs when water is lost from the concrete to the surrounding atmosphere while autogenous shrinkage occurs due to chemical reactions (chemical shrinkage) caused by the hydration process. It is important to note that both autogenous and drying shrinkage occur due to the same mechanics (disjoining pressure and capillary stress caused by the meniscus that is created between vapor filled space and fluid filled space).

The vast majority of the literature over the last century deals with drying shrinkage; however autogenous shrinkage has been more widely studied in the last two decades due to the increased use of low w/c high strength concrete and valuable information is available in publications like the Reunion Internationale des Laboratoires et Experts des Materiaux (RILEM) Technical Committee 181 report on early age cracking in cementitious systems (RILEM 2003).

There are two main differences between drying and autogenous shrinkage that should be noted. First, drying shrinkage occurs when water is lost to the environment, which can be a slow process that is dominated by non-linear diffusion (Bazant and Najjar 1972). As such, moisture gradients develop in the material with more shrinkage occurring at the surface of the material than that which occurs in the core. This is not the case with autogenous shrinkage which occurs uniformly across the cross section. Further, unlike drying shrinkage which is related to diffusion, autogenous shrinkage is related conceptually to a combination of pore size distribution and the chemical shrinkage (extent of hydration) that has taken place for a given material. Second, autogenous shrinkage increases as the water to cement ratio decreases or as finer cements (or supplementary material) are used. It is generally assumed that this can become more important in specimens with water to cement ratios below approximately 0.42; however, this is a somewhat arbitrary limit.

Figure 5 illustrates how volumetric changes can result in cracking. If the concrete were unrestrained (able to move freely) it would simply reduce its size and be stress free (assuming the stresses around the aggregate due to moisture gradients are not considered). However, in many applications there is a member that restrains movements and as such the concrete is not able to move freely. An example of this is a concrete wall on a stiff foundation and cracking would occur primarily where the restraint is highest (i.e., along the footing of the wall) (ACI 2007). In this case the foundation would restrict the movement of the wall and the bottom of the wall would be restrained from moving freely. It is assumed that, if this type of cracking would appear in the vaults, the restrained shrinkage cracking would occur along the base or in the corners of the vaults where the degree of restraint is higher.

The stresses that are developed due to restraint may or may not lead to cracking, however, as this depends on the relationship between the stress and strength. The time-dependent strength development is compared with the time dependent residual stresses that develop in Figure 5a. Cracking can be expected to occur when these two lines intersect (i.e., the stress equals or exceeds the strength). Similarly, it follows that if strength of the concrete is always greater than the developed stresses, no cracking will occur. This may not be exactly true for two reasons. First, viscoelasticity can

result in stress relaxation (Weiss et al. 1998), and second, sustained loading can result in failure at a lower stress level (Attiogbe et al. 2004).

To better understand the role of viscoelasticity, Figure 5b can be used. Instead of computing the stress that develops directly by multiplying the free shrinkage by the elastic modulus (i.e., Hooke's Law) stress relaxation needs to be considered. Although stress relaxation is a visco-elastic response that is similar to creep, creep can be thought of as the time dependent deformation due to sustained load, and stress relaxation is a term used to describe the reduction in stress under constant deformation.

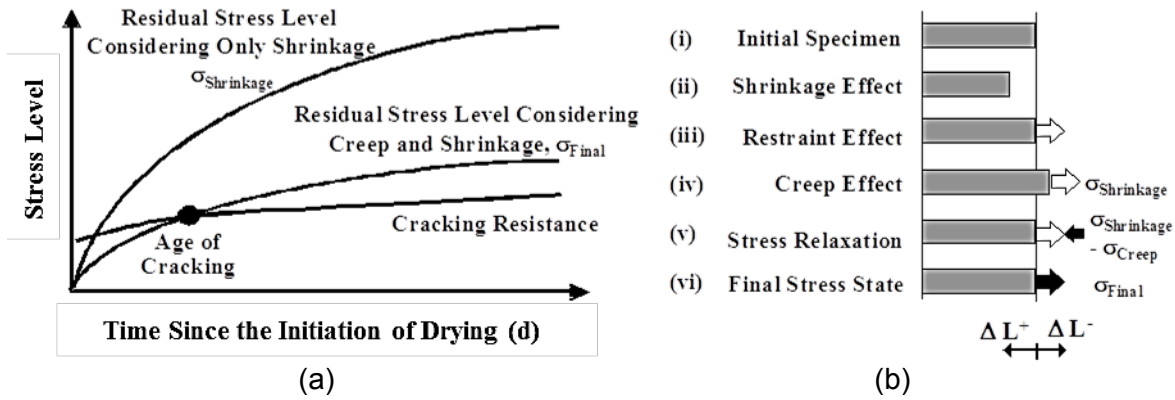

Figure 5- (a) Stress development and (b) conceptual description of relaxation (after Weiss 1999).

Figure 5b shows a specimen of original length (i) that is exposed to a uniform volumetric strain (i.e., shrinkage) that develops across the cross section. If the specimen were unrestrained, the applied shrinkage would cause the specimen to undergo a change in length (shrinkage) of (ii). To maintain the condition of perfect restraint (i.e., no length change) a fictitious load can be envisioned to be applied (iii). However, it should be noted that if the specimen were free to displace under this fictitious loading the length of the specimen would increase (due to creep) by an amount (iv). Again, to maintain perfect restraint (i.e., no length change) an opposing fictitious stress is applied (v) resulting in an overall reduction in shrinkage stress (vi). This illustrates that creep can play a very significant role in determining the magnitude of stresses that develop at early ages.

Shrinkage cracking is dependent on several factors including the free shrinkage (rate and magnitude), time dependent material property development, stress relaxation (creep), strength, structural geometry, and the degree of structural restraint (Weiss 1999).

4.4 Volume Change Caused By Temperature Effects

Concrete temperature rises during the initial hydration. However, after the first few days the temperature of the concrete is primarily influenced by the ambient temperature. Similar to the stresses that develop when hygral volume changes are restrained (see Section 4.3, "Volume Changes Caused by Drying and Autogenous Shrinkage"), when temperature changes are restrained stresses can develop and can cause cracking. The coefficient of thermal expansion in the concrete is influenced by the coefficient of thermal expansion of the aggregate since it can occupy approximately 70 % of the total volume of concrete and the coefficient of thermal expansion is known to cover a relatively wide range depending on the composition of the aggregate. For further information on designing mixtures to have a lower susceptibility for thermal cracking, documents from ACI Committee 207 (ACI 2007) or RILEM Technical Committee 172 (RILEM 1999) provide thorough treatment of this subject. The coefficient of thermal expansion is generally higher for cement paste than the aggregate.

4.5 Freezing and Thawing

Field experience has shown that properly air-entrained concrete with sufficient strength demonstrates sufficient resistance to cycles of freezing and thawing. However, under extremely severe conditions even air entrained mixtures of concrete may suffer damage from cyclic freezing (Li et al. 2012). It should be noted, however, that it is rare for concrete to reach complete saturation. Rather, work by Fagerlund (1977) and work by Li et al. (2012) have shown that concrete below a critical limit (approximately 80 % to 88 % saturation which varies slightly apparently depending on the composition of the concrete) is resistant to freeze thaw damage while concrete with a degree of saturation over 88 % will exhibit substantial damage even if it is properly air entrained (Figure 6). Air entrainment helps to substantially reduce the degree of saturation for the concrete. It should be noted that when freeze thaw damage does occur it happens more uniformly throughout the material and is not limited to a localized region like that typical for mechanically induced loading (Yang et al. 2006).

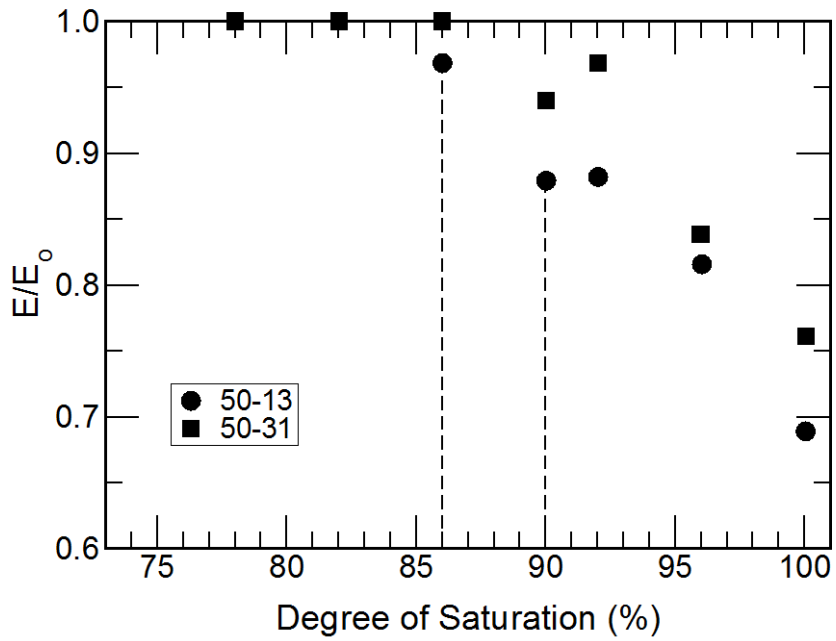

Figure 6- Relationship between stiffness degradation (E/E_O with 1.0 being undamaged) and the degree of saturation for non-air entrained (circles) and air entrained concrete (squares) (after Li et al. 2012).

If the concrete vaults will be buried below the frost line, the potential for freeze-thaw damage after burial is very, very low. However, it should be noted that prior to burial the vaults may be exposed to wetting and freezing events. For this reason it is suggested that air entrained concrete should be used for these applications. It is also believed that due to the geographical location of SRS that a relatively low number of freeze thaw cycles would be expected for these vaults, which should be confirmed with local practice. During a period of a few years it is unlikely that the concrete would experience freeze thaw damage even in locations like the bottom of the vaults where standing water may be present, which could act to increase the degree of saturation for the concrete. However, if this is a concern, the vaults could be covered or pumped to reduce the potential for standing water since standing water could increase the level of saturation in the concrete.

4.6 Corrosion

Typically, reinforcing steel in concrete is protected from corrosion by the high pH of the pore solution caused by the calcium hydroxide and the soluble alkalis. Under these high pH levels corrosion is resisted by the development of a passive layer of ferric oxide that develops on the reinforcing steel.

This passive layer prevents corrosion from occurring. If this passive layer breaks down due to carbonation, ingress of oxygen, or the ingress of chloride ions, the reinforcing steel will begin to develop active corrosion. For corrosion to initiate, moisture and oxygen must be present.

The corrosion products are expansive in nature and effectively pressurize the concrete around the reinforcing steel. Once sufficient corrosion has occurred, splitting cracks typically develop and a loss of bond is observed. The thickness of corrosion products required to cause cracking is proportional to the cover thickness. For concrete with a cover thickness of 40 mm, a corrosion thickness of 50 μm is typically sufficient to cause cracking. These cracks frequently propagate to the surface resulting in concrete spalling or loss of bond. Recent research has illustrated that preexisting cracks can accelerate corrosion initiation and propagation (Bentur et al. 1997, Yoon et al. 2000a) while sustained load further accelerates corrosion and can be sufficient to result in creep rupture (Yoon et al. 2000b).

4.7 Alkali-Aggregate Reaction

Alkali-aggregate reactivity (AAR) is caused by a reaction between specific aggregates and alkali hydroxides that are typically provided by the cement (or supplementary material) or from outside sources, such as deicing salts, ground water, and sea water. If the aggregates are siliceous, the reaction is generally referred to as alkali silica reaction (ASR), and if the aggregates are dolomitic carbonate, the reaction is known as alkali-carbonate reaction (ACR). The reaction generally causes a portion of the aggregate to dissolve or crack and an expansive gel to form which causes internal pressure to develop in the concrete (Stark 1980). When this pressure is high enough the matrix may crack leading to map or pattern cracking. This is typically a well distributed crack network throughout the concrete.

4.8 Cracking in Reinforced Concrete Elements

Cracking is generally considered in the design of reinforced concrete elements. Design equations have been developed over the years to limit crack width primarily through the amount, distribution, and location of the reinforcing steel. This report is not intended to provide information on design procedures such as those outlined in reinforced concrete texts or model codes like ACI 318 (ACI 2011). Rather, this section is intended to illustrate one important feature of cracks that occur in steel reinforced concrete. This can be illustrated using the images shown in Figure 7. Figure 7a illustrates how cracks that are perpendicular to a reinforcing bar, such as those starting at the surface of a reinforced concrete element loaded in tension or flexure, interact with the reinforcing bar. It can be noticed that in addition to opening across the bar, the crack tends to propagate along the bar causing debonding. The lugs on the reinforcing steel help to provide mechanical bond with the concrete, however, cracks form along the bar and the bar can separate slightly from the matrix. Figure 7b shows experimental results obtained from image correlation by Pease et al. (2010) who examined the role of cracking in reinforced concrete elements. Specifically it was noted that the primary crack that develops is perpendicular to the surface. Many researchers focus on this perpendicular crack when the crack is measured at the surface. However, it should be noted that as loading progresses a secondary crack develops that allows rapid lateral crack growth (debonding) along the bar that can also lead to fluid transport and corrosion. Figure 7b illustrates experimental measurements of strain taken from a cracked reinforced concrete element tested in flexure (the lower surface is the tensile face of the beam, and the horizontal reinforcement is located along the center of the image). During service loads, separation between the concrete and steel was observed to be approximately 0.1 mm nearly 50 mm away from the primary crack. It can also be noticed that the cracks that cross over the reinforcing bar (labeled as branch cracking) are greater in number and narrower than the original crack (primary crack). Using a specially instrumented rebar, Pease et al. (2010) noted that corrosion occurs along a large segment of the rebar where debonding takes place when the samples were mechanically loaded in flexure. Similar debonding and corrosion along the bar at the areas of transverse cracking has been observed by Raoufi and Weiss (2012) for samples where restrained shrinkage cracking occurred.

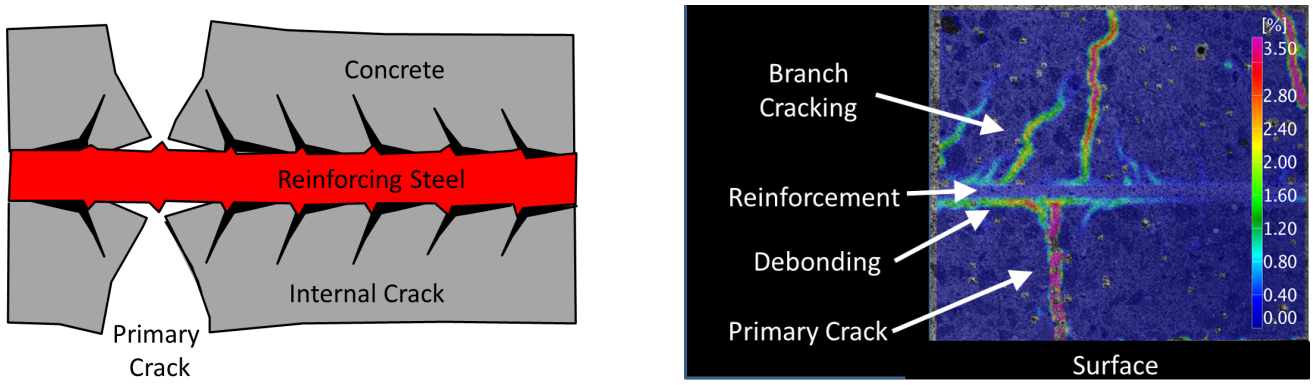

(a) (b)

Figure 7- An illustration of the role of cracking perpendicular to reinforcing steel and the accompanying debonding that occurs along the reinforcing bar: a) Illustrated conceptually (after Goto 1971) and b) Measured experimentally using image correlation (after Pease et al. 2010).

It should be noted that while Figure 7b shows actual data from a specimen loaded in flexure. Flexural cracks tend to be larger at the surface and become narrower as one moves away from the surface. Figure 8 illustrates cracking that may occur due to more of a tensile loading condition where the crack is generally uniform in width across the section but is narrower at the reinforcing bar due to bonding and pull out of the rebar. It also indicates that while several degradation processes develop at the outer surface, the surfaces of prominent cracks may also be exposed to attack.

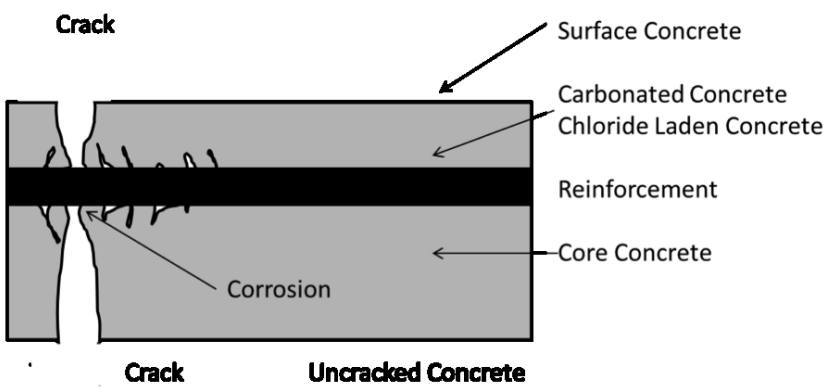

Figure 8- An illustration of a through crack in a reinforced concrete element (after Bernard and Brühwiler 2003).

4.9 Sulfate Attack

Sulfate attack can be caused by a reaction between dissolved sulfate ions in the pore solution and the AFm phases (Taylor 1990) (e.g., monosulfate) in the cement paste. The molar volume of the reaction product, ettringite, is significantly greater that the total molar volume of the reactants, resulting in expansive mechanical stress. The most common form of sulfate attack occurs through infiltration of ground water that contains sulfate. As a result, the stresses build in layers parallel to the surface, and the layers “peel off” like an onion. As each layer peels off, the attack renews at the newly exposed

surface. In addition, the calcium hydroxide can also be dissolved at the surface and magnesium from magnesium sulfates can replace the calcium in the calcium silicate hydrates.

An internal sulfate attack can occur from materials incorporated in the concrete at the time of mixing, including sulfate rich aggregate or excess gypsum added to the concrete. Delayed ettringite formation (typically a result of early hydration at elevated temperatures) can also be thought of as internal sulfate attack.

In general, external sulfate attack is most severe at the surface. This region will consist of successive damage layers that penetrate from the surface of the concrete. Each layer consists of a distributed type of cracking that, along with the expansion of the paste, causes loss of bond with the aggregate. The reaction is also dependent on presence of water (e.g., relative humidity), which is required to transport the reacting species through the paste.

4.10 Summary

In summary this section has provided a brief overview of different types of cracking that may occur in concrete elements. It should be noted that while this chapter does not provide a complete review of all cracking it hopefully does point out that the cause of cracking can have a significant influence on the morphology of the cracks that form which will influence transport. The visible cracks that form due to plastic shrinkage, restrained shrinkage or mechanical loading are generally ‘localized in nature’. The cracking that occurs from moisture gradients, freezing and thawing, and alkali aggregate reaction are generally well distributed throughout the matrix.

5 MODELING SERVICE LIFE

Because the redox potential changes relatively little (due to oxidation) until the reductant is exhausted, measuring the redox potential alone will probably not give a complete picture of the overall performance of the facility. Moreover, the redox potential will vary spatially throughout the waste form monolith, so a sufficient number of chemical sensors would be needed. A more complete picture will require information about the oxidation contributing events that were enumerated above. For example, if one knows the rate of groundwater influx through the concrete vault, the concentration of dissolved oxygen in the groundwater, and the oxygen diffusion coefficient of the waste form monolith, one could predict the distribution of redox potential throughout the waste form monolith. Converting the groundwater influx data to an "oxygen delivery" number would require some conceptual model for transport through the concrete vault.

In those cases where the waste form grout has changed (e.g., wetting/drying, cracking), the resultant "oxygen delivery" throughout the waste form grout will also require a conceptual model. The oxygen transport through the pores will occur through both the water-filled and the dry pores, and through any cracks that have formed. These scenarios will also require a conceptual model.

In the event that sufficient oxygen has penetrated the monolith that the reductant has been consumed, there could be increased radionuclide transport out of the monolith, and through the vault, into the environment. Although this scenario has similarities to the oxygen ingress scenario, it is assumed that the radionuclides must be transported within a liquid phase, and the transport of a liquid is different from the transport of a gas. This process would also require a conceptual model.

A comprehensive service life model for the entire process, from oxygen ingress to radionuclide release, would most likely be based on a physico-chemical approach of modeling the relevant transport and reaction mechanisms. The models based on physical processes have a certain commonality, and they differ in the degree to which they consider the different details. Generally, there are four components to these models:

- Characterize the environment
- Characterize the material
- Characterize transport
- Identify possible chemical reactions

For waste vaults and grout monoliths, the critical transport coefficients will be the transport properties: permeation and oxygen diffusivity. Both of these will then depend upon the moisture content of each structure.

Few, if any, service life models for cementitious materials include redox reactions. The development of service life models for cementitious materials is a challenge due to limited kinetic data for the redox reactions.

6 CHEMICAL STATE SENSORS & NDT METHODS

6.1 Moisture/Water Content

Moisture transport through concrete depends on the volume of pores, the connectivity of the pores, and the degree of saturation of the bulk concrete (i.e., water content). Generally, saturated concrete has a greater ion diffusion coefficient and a lower gas diffusion coefficient than partially saturated concrete. This follows naturally from the more available paths for ion diffusion and fewer available paths for gas diffusion in saturated concrete than unsaturated concrete. As the moisture/water content changes in a concrete, so will the ion and gas diffusion coefficients.

There are two approaches to estimating the water content of concrete. The direct method is to detect the change in the concrete properties as a function of the volume of water that is present. The indirect method is to measure the relative humidity that is in equilibrium with the concrete and combine this information with the adsorption-desorption isotherm to estimate the moisture content.

Time domain reflectometry (TDR) is a viable direct measurement of water content. In this test, the probe is an antenna that is in intimate contact with the material of interest. A very short pulse is propagated along the probe, and the reflected signal is analyzed. The reflected wave amplitude and phase, and the apparent wave speed, depend upon the dielectric properties of the medium surrounding the probe. As has been done for soils (Topp et al. 1980), the relationship between the bulk dielectric property and the moisture content would have to be established as part of a separate experiment (Mollo and Greco 2011). The TDR technique can also be combined with a coaxial-cable crack sensor embedded in a full-scale reinforced concrete for dynamic structural analysis (Bishop et al. 2011). The disadvantage of TDR is that the technology has not been demonstrated conclusively for all types of concrete materials, and the very high conductivity of the salts remaining in the pore solution of saltstone may cause measurement challenges. Therefore, tests are needed to demonstrate and calibrate this technique on saltstone, tank backfill grouts, and vaults.

The electrical conductivity is another direct means of estimating the water content. The electrical conductivity of a concrete is a strong function of the concrete moisture function, assuming that only water enters and exits the concrete microstructure. The electrical conductivity can be estimated using non-corroding electrodes placed into the concrete. There could be multiple pairs of electrodes, and the electrodes could be arranged so that one could also estimate a water content profile (Weiss et al. 1999). The measurement is performed by applying a sinusoidal voltage and measuring the phase and the amplitude of the resulting current. The relationship between bulk electrical conductivity and moisture content would have to be established as part of a separate experiment. The disadvantage of this approach is that concrete conductivity is affected by a number of factors (e.g., continued hydration), and once multiple factors occur, it may be difficult to identify the precise cause of changes in conductivity.

For indirect methods of estimating water content, one of the most accurate ways to measure relative humidity is the chilled mirror hygrometer (CMH). In the CMH setup, a light source is reflected at an acute angle off a mirror having a front surface reflective coating. The sample gas passes over the mirror, and the temperature of the mirror can be controlled precisely. When the mirror temperature falls below the dew point of the sample gas, moisture condenses on the mirror, scattering the reflected light. Measuring the temperature of the incoming gas and the dew point temperature are sufficient to determine the relative humidity of the sample gas. For this method to work, the gas must be circulated, requiring a power source. The disadvantages to this method are that there must be gas circulation, reliable temperature control, and the mirror requires periodic cleaning.

A more convenient approach to measuring relative humidity is to use a moisture-sensitive capacitive element in an oscillatory circuit. The capacitor is created by filling the space between two metallic electrodes with a polymeric material with a monotonic adsorption-desorption isotherm. The moisture content changes the dielectric, which changes the capacitance. The natural frequency of the oscillatory circuit can be related to the relative humidity by using standard saturated salt solutions (Greenspan 1977). A disadvantage of this method is that the capacitive element requires periodic re-calibration, and the long-term reliability of these sensors has not been demonstrated.

Another indirect approach to estimating moisture content is to use a tensiometer. These devices measure the degree to which water is being “held” by a material (typically used in soils). A partially saturated material that is hydrophilic will generate fluid menisci with negative curvature, meaning the fluid is under a negative pressure, with respect to the atmosphere; a saturated soil can have menisci with positive curvature and a positive fluid pressure. The tensiometer measures this pressure, and the limits of commercially available tensiometers vary from +100 kPa down to -160 kPa. A tensiometer is typically composed of a ceramic cup, plastic tubing, a stopper, and a pressure transducer (Young et al. 1999).

There are a number of standardized tests for characterizing the moisture content and vapor transport coefficient of cementitious materials:

ASTM F1869 Standard Test Method for Measuring Moisture Vapor Emission Rate of Concrete Subfloor Using Anhydrous Calcium Chloride.

ASTM F2170 Test Method for Determining Relative Humidity in Concrete Floor Slabs Using in situ Probes.

ASTM F2420 Standard Test Method for Determining Relative Humidity on the Surface of Concrete Floor Slabs Using Relative Humidity Probe Measurement and Insulated Hood.

6.2 pH

The pH of the pore solution within a cementitious material reveals a lot about the chemical state of the system. As the cementitious materials hydrate, they release alkalis (primarily potassium, sodium, and calcium) into the pore solution. The calcium reacts with silica to form a poorly ordered calcium silicate hydrate (C-S-H) that is the primary binding phase. The potassium and sodium remain in the pore solution: a small fraction is bound within the C-S-H. If the concrete comes into contact with a solution having a lower alkalinity, the alkalis in the pore solution can be leached from the concrete; the alkalis bound within the C-S-H will also be released into the pore solution to achieve a thermodynamic equilibrium.

A pH probe measures the electrochemical potential between a sample solution and an internal solution (typically KCl). The internal solution is separated from the sample solution by a thin porous glass membrane that is coated (inside and out) with a very thin gel. The gel exchanges Na^+ for the H^+, and the Na^+ ions are transported through the glass membrane. An additional reference electrode, having a separate buffer solution and exchanging solution (via a porous glass membrane), complete the circuit. A high impedance multimeter is used to determine the voltage between the two electrodes within the pH probe, and the device is calibrated using standard solutions.

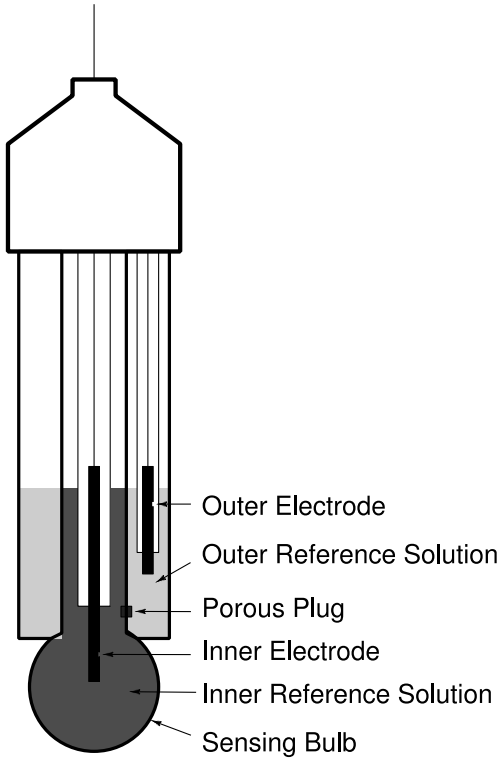

Figure 9- A schematic of a combination pH electrode (adapted from Ritz and Collins 2008).

Available pH electrodes have limitations in field environments. The limitations are related to the species present and whether the probe can be serviced to maintain functionality and calibration. A list of potential pH electrodes for specific environmental conditions is given in table 2 below.

Table 2- pH electrodes recommended for water having elevated concentrations of sodium and other monovalent major cations and sulfides (Ritz and Collins 2008)

Chemical Condition	Description of Water	Degradation Effect (Combination pH Electrode)	Recommended pH Electrode
Basic ions dominant in solution	pH high (>10 pH units); low H^+ activity results in measurement of other monovalent ions in solution.	Sluggish response to changes in pH, resulting from dehydration of the glass membrane.	Glass pH electrode designed for measuring high values of pH.
	Sodium effect: Elevated Na^+ at pH above 11, H^+ activity is low. The electrode senses Na^+ activity as if it were H^+ because of the similar charge and structure of the Na^+ and H^+ ions.	The pH measurement is negatively biased.	Glass pH electrode designed for measuring high values of pH.
Elevated concentrations of sulfide or cyanide	Elevated concentrations of sulfides or cyanides are found in industrial, mined, or urban areas.	Sulfide or cyanide contamination of the internal reference electrode.	Double-junction electrodes and plasticized reference electrodes.

From a practical perspective, the long-term use of a pH electrode would have severe limitations. Liquid-filled combination electrodes would require periodic flushing to restore the solution to a known concentration. Gel-filled electrodes are an alternative because they do not require filling and typically require less maintenance than liquid-filled electrodes. Unfortunately, they are not a permanent solution because the gel-filled electrodes can also change composition over time through leaching in pure water or adsorption in concentrated solutions (Ritz and Collins 2008).

A relatively new technique using an acid-base indicator may show promise. The pH sensor consists of trinitrobenzenesulfonic (TNBS) acid, which is the indicator. The acid is prepared in a sol-gel, and is then coated on the surface of glass. (The glass could be a fixed element or a fiber optic strand.) The optical properties of the TNBS acid change in the pH 12 to 14 range, and any changes in the optical properties can be detected using a light emitting diode (LED) and photodiode. The technique has been demonstrated in the laboratory. As long as the indicator remains in the sol-gel, the sensor remains accurate; no periodic calibrations are required. Although it has been postulated that the technique can be used in concrete (Srinivasan et al. 2000), there are no data on the long-term performance.

6.3 Redox Potential

Redox potential is measured using a reference solution and two electrodes, and is a measurement technique commonly used to characterize soils. To perform the measurement, a metallic sample electrode is placed into the material being tested, and a reference electrode is electrically connected (e.g., a salt bridge) to a reference solution with a reference electrode (e.g., calomel or Ag/AgCl) (Schüring et al. 1999). (The reference electrode can be incorporated into the housing containing the sensing electrode) The sample electrode is typically made by fusing platinum (Pt) to a shielded copper wire. An excellent discussion of these measurements can be found in Nordstrom and Wilde (2005). Conceptually, it is very similar to measuring pH, with the main difference that the sampling electrode is a metal rod.

The instrumentation consists of measuring the electrical potential between the two electrodes. The reference half-cell will have a known potential drop, which is subtracted from the measured value to obtain the redox potential. Although there is also a voltage drop at the Pt electrode, the properties of soils have been characterized by the potential observed by the Pt electrode.

One of the biggest challenges with leaving the electrode in the sample for a long time is the robustness of the electrode surface. Hydrogen sulfide can contaminate Pt and Au electrodes, which would require routine cleaning (Langmuir 1997, Nordstrom and Wilde 2005), even after just a few hours (Whitfield 1974). This would be very relevant to saltstone waste forms containing blast furnace slag.

There has also been work using carbon-based electrodes. The most commonly used carbon-based electrode in the analytical laboratory is glassy carbon (GC). It is made by pyrolyzing a carbon polymer, under carefully controlled conditions, to a high temperature like 2000° C. McCreery (1999) provides a thorough review of a number of types of carbon-based electrodes. Although these electrodes are considered very inert, activating the surface can be challenging. However, because a recommended storage condition is a solution of alumina or silica species, they may be viable long-term electrodes for cementitious systems. Wikberg (1985) has reported on the use of carbon electrodes to measure the redox potential E_h in a bore-hole, and a similar, more recent report on the use of glassy carbon electrodes was given by Laurent (2008). Švancara et al. (2009) has provided a more recent review of advances in carbon electrodes for electrochemical applications.

Relevant standardized tests for redox potential exist for soil testing and measurements made in the laboratory:

ASTM G200 - 09 Standard Test Method for Measurement of Oxidation-Reduction Potential (ORP) of Soil

ASTM D1498 - 08 Standard Test Method for Oxidation-Reduction Potential of Water

6.4 Radionuclide Detection

Detecting the presence of mobile radionuclides within the vault will be challenging. Effective detection requires a preconcentrating column, and remote sensing will require scintillation (Grate et al. 2008). Although polymeric beads with both ion-exchange and scintillation properties were discovered in the 1960's (Heimbuch et al. 1965), only relatively recently have researchers created dual-acting polymeric beads for detecting ^{99}Tc in water (Egorov et al. 1999). Although there may be promise for sensing in long-term applications, the detection of mobile radionuclides is an indication that a problem already exists.

7 STRUCTURAL HEALTH MONITORING

The process of implementing a damage detection strategy for engineered systems is referred to as structural health monitoring (Farrar and Worden, 2007a; Farrar and Worden, 2007b). While structural health monitoring uses traditional methods such as vibration-based methods, the methods discussed in this report are designed to focus more on a performance assessment of a containment facility and its prognosis for anticipated service. It is important to identify health monitoring techniques that can be used for damage identification (i.e., time, location and extent of damage) and the measurement of the influence of damage on transport. It is also important to utilize sensors for identifying parameters like the degree of saturation or pore solution properties that can dramatically influence redox and transport. Furthermore, a portion of the information gathered should be used to assess damage prognosis which is defined as "the coupling of information from the system's original design, loading environments, health monitoring, usage monitoring, past-current-anticipated future environmental and operational conditions, previous component and system level testing, and numerical modeling to estimate the remaining useful life of the system" (Farrar and Lieven, 2007).

Cracks can occur in concrete elements for a variety of reasons. These cracks can be important to nuclear waste containment facilities due to the potential influence of cracking on accelerated liquid, gas, and contaminant transport. Figure 10 illustrates the three aspects of the problem that need to be understood to better quantify the role of cracking on the transport properties of concrete elements (Weiss et al. 2007). Figure 10a describes the importance of understanding the cause of cracking since this can have a significant influence on the type of cracking that can occur. Figure 10b illustrates the need to better understand the geometry and morphology of the crack network. While this may originally just be thought of as crack size, it also includes aspects of crack distribution, connectivity, and access to the surface of the concrete element. Figure 10c illustrates the need to assess the influence of cracks and moisture conditions on transport that can then be used to assess the influence of cracks on long-term durability performance of a concrete structure. This can include the role of fluid transport through cracks while the concrete and crack can be unsaturated or saturated (Langton and Weiss 2012). The potential uses of health monitoring concepts for implementing a damage detection plan are two-fold: 1) determine whether cracks have developed, and 2) determine the potential influence of the crack network on fluid, gas or contaminant transport.

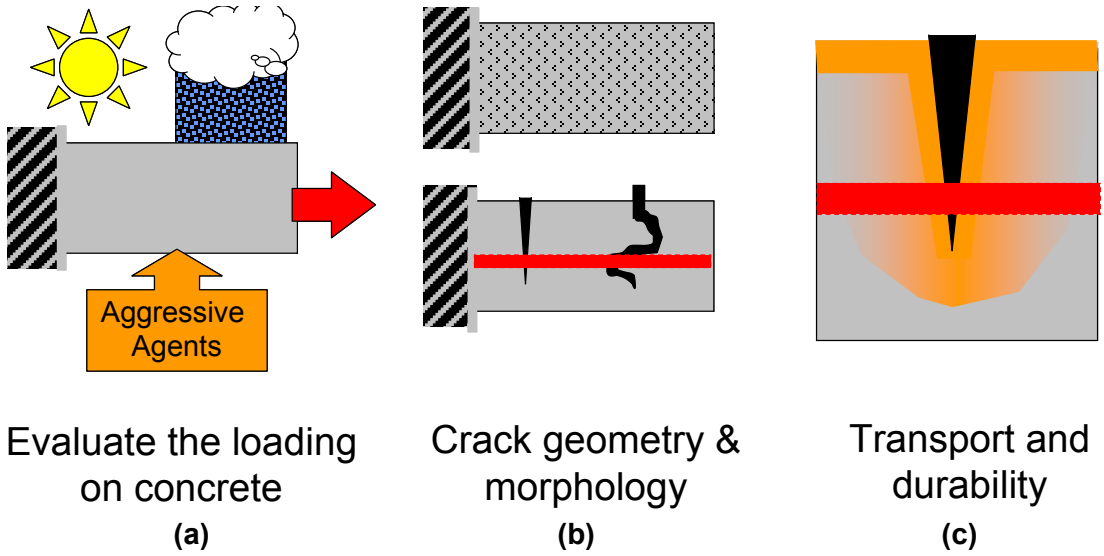

Figure 10- A schematic of how crack formation can influence transport processes in concrete: a) environmental causes of cracking, b) distributed (micro-cracks) and coalesced cracks, and c) pathways for both ingress and egress of moisture, gases, and dissolved species.

In the following section, the most viable health monitoring methods are discussed in the context of assessing cracking and its potential influence on transport: 1) acoustic emission, 2) electrical resistivity of the bulk concrete, 3) electrical resistivity of surface skin elements, 4) magnetic sensors for monitoring opening (for joints or cracks), 5) visual, thermal or shearography and 6) ultrasonic transmission. Each technique is discussed in the context of its potential use in grouts for waste solidification and concrete for containment vaults.

8 STRUCTURAL HEALTH MONITORING TECHNIQUES

8.1 Acoustic Emission

Acoustic emission (AE) is a field of study that consists of a class of non-invasive experimental techniques that are founded on the principle that the formation of damage in a material results in the release of an elastic energy wave (Scott 1991). Frequently this energy release occurs in the audible range, resulting in the 'cracking sounds' that are heard during catastrophic failures. While human ears can detect large-scale failure events, piezoelectric transducers are required to detect the microscopic events associated with the release of energy (in both the audible and inaudible range) during initial crack formation and propagation. These events result in a vibrational wave that propagates through the system. When these waves reach a sensor that has been attached to a specimen, the vibrations are amplified and recorded for further characterization and analysis. While sound has been used to assess damage in materials for centuries dating back to potters and copper craftsman, recent work over the last several decades has focused on quantifying and analyzing these events in a completely new way. Recent studies have shown that acoustic emission can be used to detect and locate cracking in concrete caused by mechanical loading, corrosion, restrained shrinkage, freezing and thawing and alkali aggregate reaction (Weiss and Olek 2005, Pour Ghaz et al. 2012).

It is important to note that acoustic emission differs from many other nondestructive techniques in that it does not actively input a stimulus and record the response of the material to this stimulus. Rather, acoustic emission is a passive technique that listens for emissions that develop in the material itself during loading. While acoustic emission is a powerful method to assess the development of damage, it is frequently difficult to perform quantitative analysis on a structure that is in service due to sounds that are generated during the operation of the structure. This would be particularly true of a structure that houses operating mechanical equipment. By contrast, waste isolation vaults should be free of any such mechanical interference.

Previous studies have shown that acoustic emission can be used to detect the onset of cracking and to locate the cracks in the concrete element. Location is estimated using triangulation by measuring the differences in the arrival times for the wave at different sensors. In addition, this may provide some indication of the spatial distribution of damage, which may provide insight into the cause or extent of cracking. Figure 11 shows results of a recent study to assess the size of the damage zone for freeze thaw damaged samples that were tested in tension (Yang et al. 2006). In these studies, the metric of damage is the relative elastic modulus E/E_o, which is determined from changes in the ultrasonic pulse velocity. It can be seen that in previously undamaged samples the damage caused by mechanical loading localizes to a region approximately the size of the maximum aggregate (in this case 19 mm). As the initial freeze-thaw damage level increases, the damage is more uniformly distributed along the length of the sample. This implies that freeze-thaw damage gives rise to a crack network that is uniformly distributed throughout the sample. It should be noted that while freeze-thaw damage is not likely to occur in structures in warm climates or in structures buried below the frost line, this distributed type of damage is similar to what may be expected from sulfate attack or alkali aggregate reaction. As such, information on the distribution of damage may provide insight into the mechanisms responsible for the damage.

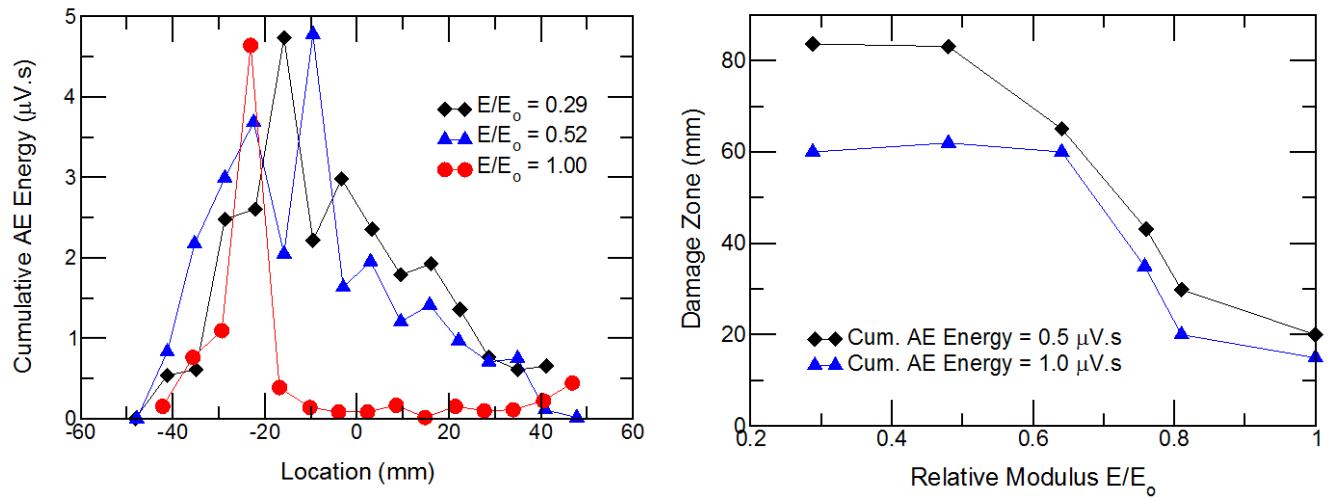

(a) (b)

Figure 11- Acoustic activity: a) the spatial distribution of activity during loading in freeze-thaw damaged samples, and b) the size of the damage zone when measured under tensile loading as freeze-thaw damage increases (E/E_o decreases) (after Yang et al. 2006).

8.2 Electrical Properties of the Concrete

The electrical properties of cement-based composites have been used to characterize crack development and damage (Bontea et al. 2000; Cao and Chung 2001; Chen and Chung 1993; Chen and Chung 1995; Chen and Chung 1996; Gu et al. 1993a; Gu et al. 1993b; Niemuth, 2004; Peled et al. 2001). Both direct current (DC) and alternating current (AC) techniques have been used for these purposes. While DC resistance measurement methods are inexpensive and easy to implement and interpret, this approach can result in electrode polarization, which can hinder accurate measurements (Macdonald and William 1987; Uhlig and Revie, 1985). An alternative to the DC current measurements is the application of a low voltage alternating current using electrical impedance spectroscopy (EIS) (Gu et al., 1993a; Gu et al., 1993b; Niemuth, 2004b; Weiss et al., 1999). Previously, EIS has been successfully applied for damage characterization and quantifying the cracking and micro-cracking in concrete and carbon fiber reinforced cement paste (Gu et al. 1993a; Gu et al. 1993b; Hou and Lynch 2009; Niemuth 2004; Peled et al. 2001; Reza et al. 2003).

Electrical measurements in concrete and cement research have been used for a wide variety of applications. Recent research has investigated the use of electrical measurements to detect cracking and to determine the influence of cracks on the transport behavior of concrete. The feasibility of using electrical measurements is illustrated in Figure 12. In the study, a cylindrical concrete specimen was made having a longitudinal crack (a sawed notch) along the outer surface of the cylinder, and the electrical resistance was measured as a function of the angle between the electrical probes and the notch. Both physical measurements and numerical simulations were performed using diametrically opposed electrode pairs that were 'rotated' to take measurements at different orientations around the specimen. The measurements were described in terms of the angle from the flaw to the position of the nearest electrode pair as shown in Figure 12b. A geometry factor (k) was computed for specimens with various cylinder diameters:

$$k = \frac{R_b}{\rho} \tag{1}$$

where ρ is the resistivity of the intact (no crack) material, and R_b is the measured bulk resistance. It can be seen from the data in Figure 12b that as the position of the electrodes is changed, the electrical resistance (or geometry factor) changes. As such, this indicates that the electrical measurements can be sensitive to the presence of cracking. The crack can be either unsaturated with the air in the crack being substantially less conductive than the concrete, or saturated and more conductive than the concrete. Figure 12b shows that for one case (air in the crack) the geometry factor is substantially higher than when the electrodes are perpendicular to the crack. It should also be noted that the case of the crack being perpendicular to the electrode path is nearly identical to the unflawed geometry until the crack becomes very deep.

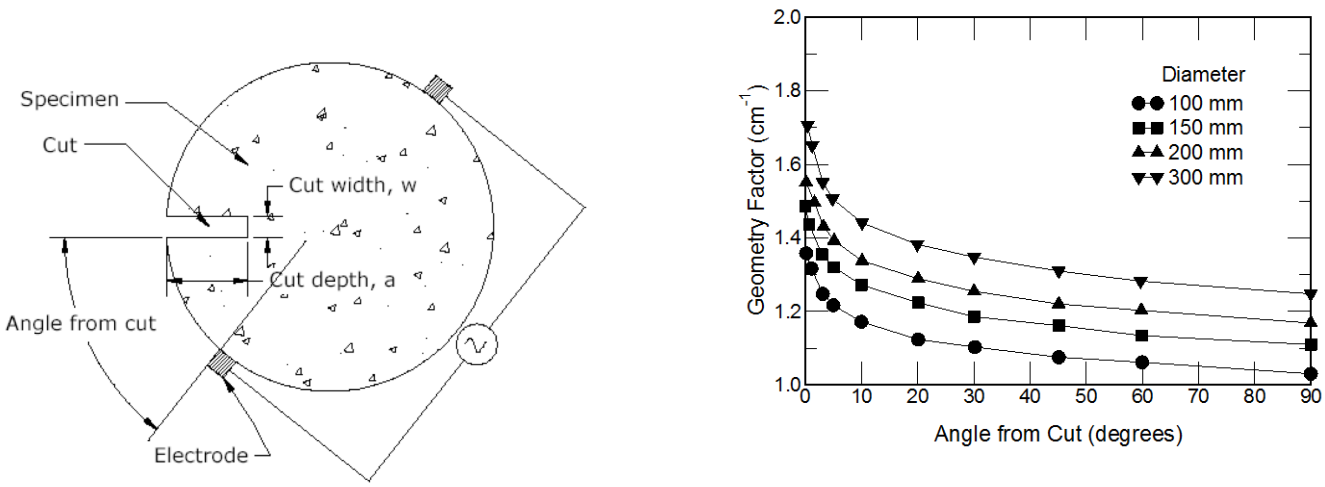

(a) **(b)**

Figure 12- Electrical response of cracked concrete: a) an illustration of the sample geometry used for electrical measurements and b) the measured electrical response as a function of crack orientation.

In addition to using the cylindrical geometry shown in Figure 12a, work has demonstrated that electrical measurements can be used to describe cracking in a slab where only single-sided access is possible. This method was quite successful in locating cracks when the damage is visible at the surface or even in cases where the crack is not visible (Poursaee and Weiss 2010).

It should be noted that measurements of the electrical properties of concrete may be influenced by the moisture content of the concrete or the presence of reinforcing bars.

8.3 Electrical Properties of Films or Surface Coatings

Since a majority of the cracks that form in concrete originate from the surface, Pour-Ghaz and Weiss (2010a) proposed that conductive surface coatings could be used as a method to detect cracking. This concept is illustrated in Figure 13. In this method an electrically conductive thin film is applied to the surface of the concrete (alternatively it may be possible to use a fiber or ribbon placed 'inside the concrete'). These films can be made of conductive epoxy, paint or conductive tape. The electrical resistance of this film is monitored as the substrate cracks.

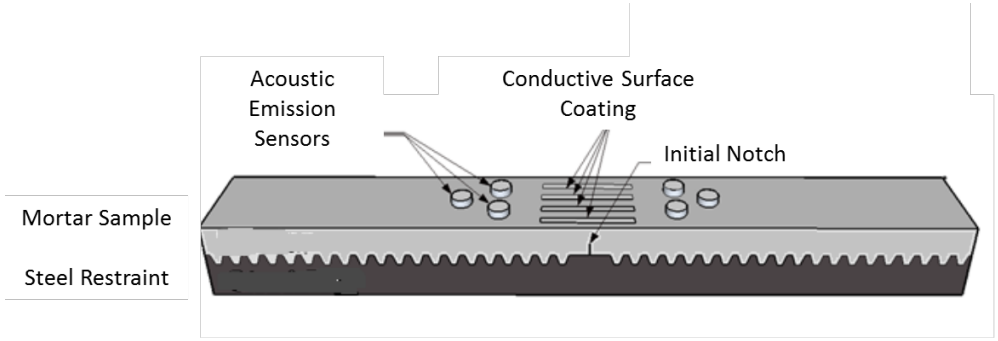

Figure 13- A conceptual illustration of acoustic emission sensors and conductive surface coatings on restrained slab elements.

Initially the electrical resistance of the conductive film increases gradually as the conductive film is stretched. When the substrate cracks sufficiently to break the conductive surface, the resistance of the conductive surface material increases dramatically and the time and location of cracks is recorded. Although the application of the technique shown in Figure 14 is for a relatively small (approximately 100 mm) element, this method has been successfully applied to elements 5 m in length, and it can be scaled to even larger dimensions.

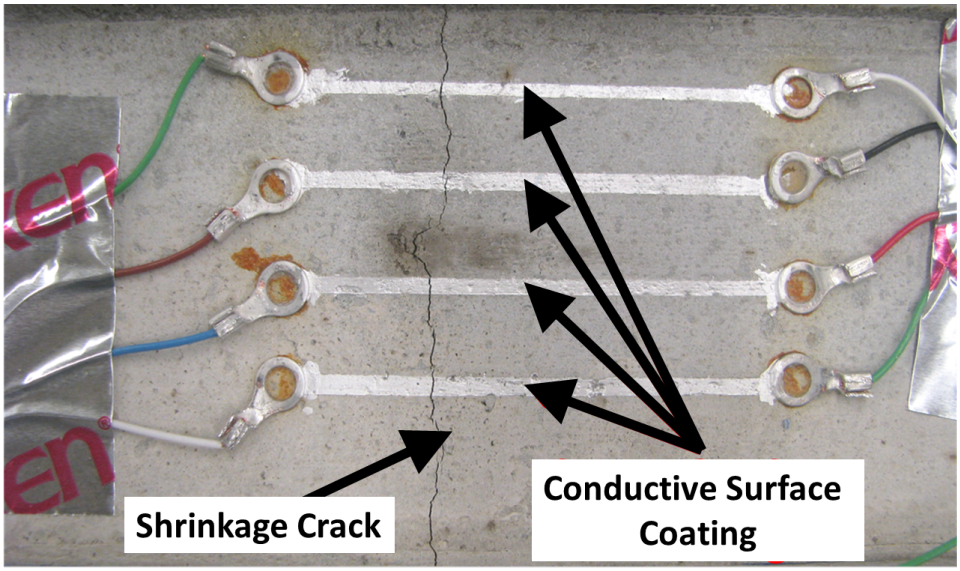

Figure 14- A typical picture of a cracked slab at the mid-span (at the notch location). The four strips of conductive surface coating and their electrical connections are also shown.

Conductive surface treatments have previously been applied to laboratory specimens, to buried pipelines subjected to permanent ground displacement, and to quantify the damage in restrained ring test samples (Pour-Ghaz et al. 2010a, b). Similar approaches have also been proposed using surface films for monitoring damage (Laflamme et al. 2012).

Two approaches have been used to quantify the relationship between strain/cracking and the electrical response of the conductive strips. The first approach used DC or AC techniques to measure the film resistance. The second approach used impedance spectroscopy to assess crack location and size. This is done using an equivalent circuit model (Pour-Ghaz and Weiss, 2011) as an extension of a switching model proposed by Mason (Hixson et al., 2001; Mason et al., 2002; Torrents et al., 2000; Torrents et al., 2001a,b).

The change in resistance of the surface film that occurs during cracking has been studied. Figure 15 shows a plot of the change in resistance of a conductive copper tape applied to the surface of the mortar and the strain that is measured, both as a function of the duration of the experiment. The time of cracking corresponds to the release of restraint and the sudden change in strain of the restraining element. The occurrence of a crack is detected by the change in the electrical resistance measurement at the time of the first strain release in the steel ring.

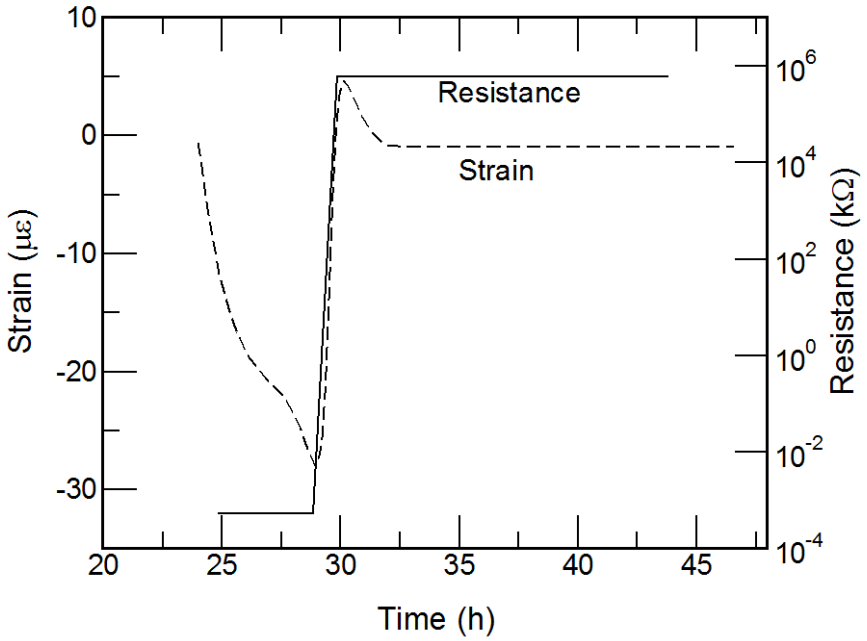

Figure 15- Time of cracking detected by monitoring the strain in steel ring and resistance increase of copper tape applied to the surface of mortar in restrained ring test (Pour Ghaz et al. 2011).

In addition to being able to detect the crack location, the approximate number of cracks in the material can be determined using different arrangements of electrodes and application of conductive surface materials. The frequency dependent response of the circuit can be used to estimate the location of cracks, to estimate the size of cracks, or to query multiple sensors using a frequency selective circuit.

8.4 Magnetic Crack Opening Sensors

Magnetic opening (MO) sensors are two-part sensors consisting of a switch and a magnet. The switch is triggered depending on the strength of the magnetic field, which is dependent on the proximity of the switch and the magnet. Figure 16 illustrates a commercially available MO sensor in which the switch is triggered when the gage opens by more than 2.5 mm. It should be noted that while this type of sensor is relatively straightforward, it does require the location of the crack/joint to be known before installation. As such this type of sensor is useful in assessing the width of an existing crack, but it is not ideally suited for a more global assessment.

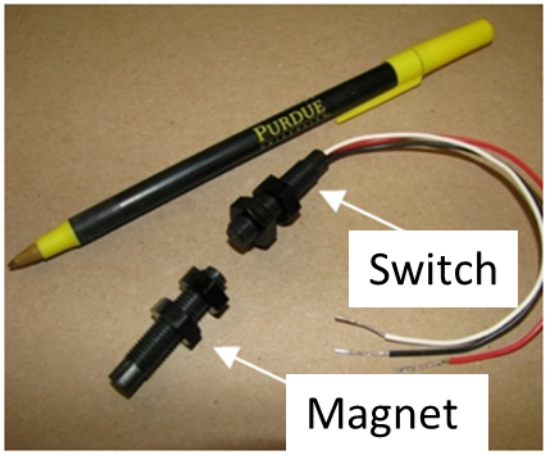

Magnetic Switch

Figure 16- Illustration of a magnetic crack opening sensor (after Pour-Ghaz et al. 2011).

8.5 Visual Imaging, Thermal Imaging, and Shearography

The first form of nondestructive testing that is typically used to inspect concrete is a visible inspection for damage, segregation, or construction defects. Because these methods are not always quantifiable and not without some measure of bias, image analysis techniques may permit the crack width to be assessed rapidly at numerous locations without such operator bias. While conventional image analysis of still images has been used for detecting surface cracks, other researchers have used thermal imaging to assess the heat release associated with the formation of cracks.

Previous reports have indicated success with infrared imaging or laser shearography (Khong et al. 2007) both of which are rapid nondestructive testing procedures that may be able to cover large areas and without contact with the surface of the concrete. A laser shearography system was developed into a portable unit through a small business research grant (SBIR) in collaboration with Federal Highway Administration (FHWA). This approach used a change in temperature to cause a movement at the surface of concrete that allowed cracks to be imaged.

8.6 Ultrasonics

Ultrasonic Pulse Velocity (UPV) is a nondestructive test that has been proposed to evaluate the internal damage, uniformity, and relative quality of concrete. The wave transmission time can be used to assess damage in concrete with a slower wave speed corresponding to cracked/damaged materials. While the presence of cracks results in a reduction in the wave speed, it should be noted that only large internal flaws or significant changes in uniformity would have a significant influence on the UPV (Suaris and Fernando 1987 and Popovics et al. 1990). This suggests that UPV techniques may be useful for locating larger cracks or flaws, but only those flaws that are sufficiently large. Recent studies of alternative uses of ultrasonic waves may provide merit for field investigations to determine where cracks may exist and where samples may need to be obtained (ACI 2012). A spectral analysis of surface waves (SASW) or a group velocity plot may be used to estimate the stiffness (or elastic modulus) of the concrete as a function of depth. This may provide a rapid field measurement of locations that demonstrate substantially lower surface waves that would indicate damage that may merit further investigation.

8.7 Geophysics

Techniques to measure the electrical resistivity of bulk geological materials have been developed that can be used to assess moisture content, ionic strength of pore water, and other properties. In its most elementary form of application, an alternating electrical current is applied between two electrodes ("current" electrodes) inserted at the ground surface while information on the induced electric field is obtained by measuring the voltage between a second pair of electrodes ("potential" electrodes) either inserted at the ground surface or down a well. The applied current, the resulting measured voltage, together with knowledge of the electrode spacing and configuration allow determination of the bulk resistivity of a subsurface soil volume. Resistivity measurements can be conducted in a variety of configurations. Useful information can be obtained from the time series of voltage values or data can be used to generate images. These can be relatively simple 2-D interrogations of a plane through the subsurface to much more complex 3-D or tomographic imaging techniques that require sophisticated computational analysis. For 3-D imaging, Electrical Resistance Tomography (ERT) is a method that calculates the subsurface distribution of electrical resistivity from a large number of resistance measurements made from electrodes on the ground surface, in boreholes, or both, to produce images of vertical or horizontal sections. Depending on the application, resistivity variations can then be related to geology, subsurface moisture content, porosity, temperature, and pore fluid chemistry.

The use of electrical methods to assess the moisture content or cracking of concrete has been studied, but samples are relatively small; only a few tens of cm or less. Seppanen et al. (2009) discuss the use of electrical resistance tomography to image concrete. Peled et al. (2001) examined the use of electrical impedance spectra to assess cracking behavior of fiber-reinforced cement. Lataste et al. (2003) used electrical resistivity to assess cracking in concrete. The use of resistivity techniques for large monoliths such as the saltstone or tank backfill grouts should require more simplified analysis than structural concrete containing rebar. It may be possible to assemble arrays of electrodes on two or more rods that are left in place in the tank as grout is added. By using various electrodes as the current sources and the potential electrodes, a complex network of measurements can be made to assess the moisture content of the grout. The measurements can be automated and run periodically so that time series data can be compared to determine if moisture is moving into the system. It may be possible to determine if areas of cracks develop by changes in the electrical properties.

8.8 Example Application: Pipeline Subjected to Ground Motion

Several of the approaches mentioned in the previous sections were applied to a buried segmental concrete pipeline that was being tested to assess damage caused by permanent ground displacement (i.e., cracking due to an earthquake) (Pour Ghaz et al. 2012). These sensors were placed on a commercial Class III/IV reinforced concrete culvert pipes with an inner diameter of 34.5 cm (12 inches). The concrete pipe was placed in a split box test basin at the Network for Earthquake Engineering Simulations (NEES) Large-Scale Lifelines Testing Facility at Cornell University. The test basin was 3.4 m (≈ 11 ft) wide and 13.5 m (≈ 44.3 ft) long and 2.3 m (≈ 7.5 ft) deep. Four methods were used to detect cracking in the concrete pipe:

1) Conductive surface tape (CST)
2) Magnetic opening (MO)
3) Acoustic emission (AE)
4) Conductive grout

A displacement-controlled testing procedure was used on the pipeline. The CST sensors showed clear indication of cracking and damage development. This showed both the time of cracking as well as the location of cracking. Before cracking, the CST sensor's resistance is approximately 0.05 Ω. After cracking, however, the resistance increases several orders of magnitude. The resistance measurements are compared to thresholds so that the condition may be expressed in binary, with a zero indicating an intact CST (i.e., no damage) and a one indicating a damaged CST (i.e., a crack below the CST). The MO sensors showed joint opening. However, it should be noted that the joint needed to be known prior to sensor placement. A significant increase in acoustic energy is observed before damage was detected using the CST or MO sensors. The sensing approaches captured the damage development in the segmental concrete pipeline, and the damage was consistent with the visual inspection after excavation of the pipeline. The sensing methods used provided the time- and location-dependent

information on damage development in the pipeline. The results indicate that these methods can be used individually or along with other methods to monitor the health and integrity of buried segmental concrete pipelines. The results indicate that acoustic emission provided information about the occurrence of damage and cracking earlier than the electrical methods used in this work.

9 POTENTIAL STRUCTURAL HEALTH MONITORING SOLUTIONS

It should be noted that two different applications are considered for potential use of these sensors in waste isolation facilities. The first application would be for monitoring the vault itself. The second application would be for monitoring the structural health of the saltstone material in the vault, or backfill grout in the tank. Potential applications and uses are described in the following section.

9.1 Monitoring the Vault

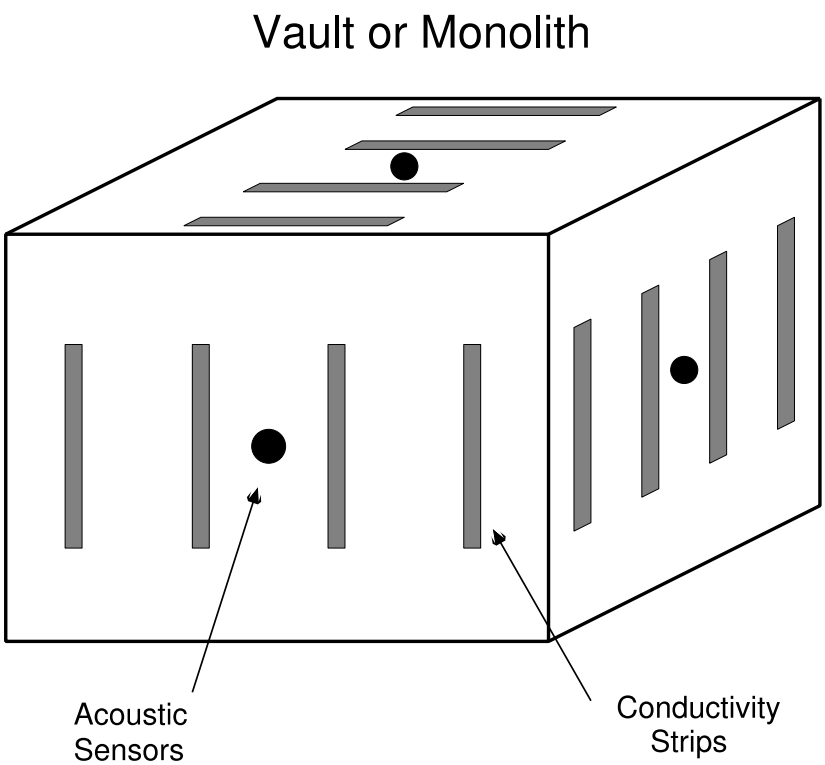

Figure 17- A schematic of how conductivity strips or acoustic sensors could be placed in an array on the surface of a saltstone monolith (or interior wall of the vault) or on the exterior surface of the concrete vault to help monitor the overall performance of the system.

There are two different approaches that can be used in monitoring the vault walls based on whether the vaults can be accessed before the saltstone is placed or whether the vaults are inaccessible.

For cases where the interior of the vault is accessible, it is possible to install conductive film and acoustic sensors directly on the surfaces of the vault, shown schematically in Figure 17. The conductive films can be arrayed to monitor the bulk transport properties of the concrete to be monitored; using electrical resistivity, the degree of saturation and the formation factor can be determined, which are related to the transport properties used in service life prediction. The combination of conductivity films and acoustic sensors can be used to detect and monitor cracking within the vault. The sensors can be brushed, sprayed or adhered to the surface and can be covered with a protective film or epoxy to minimize the potential for corrosion or degradation. In these cases it would also be possible to place acoustic sensors on either the inside or outside of the vault. These sensors could also be protected from the elements and a strong coupling could be obtained. While the exact geometry of the conductive sensors would require more study, it is quite possible to consider a grid where conductivity could be monitored using sections that are on the order of several meters long. This approach would yield a more accurate indication of the overall (average) performance of the system.

For those cases where the interior of the vault is inaccessible, a gridded framework could be developed on the external surface with a 'conductive wire' that could monitor electrical conductivity. One of the key aspects of this gridded system would be the ability to adhere the elements to the surface of the vault. This may be done through an adhesive bond or even mechanical anchorage (though this may be discouraged due to potential challenges that may arise if the vault wall is penetrated).

9.2 Monitoring the Grout

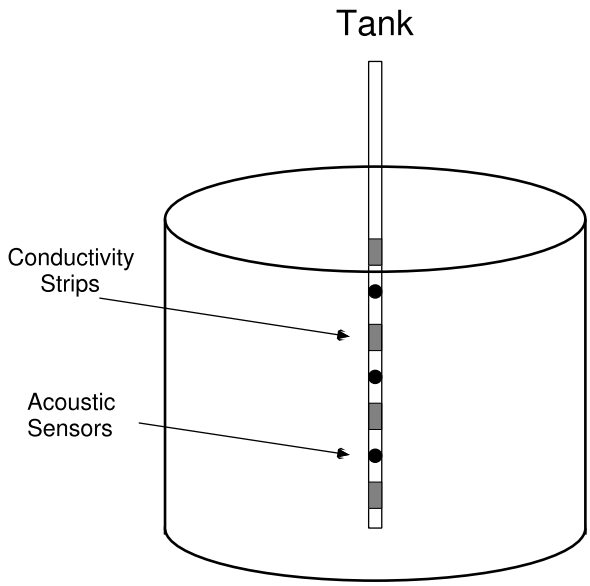

Figure 18- Schematic of a single-pole approach to installing sensors in a grout monolith during construction. A similar configuration using two or more rods, could also contain electrodes for resistivity measurements.

For cases where the vaults are accessible during construction, it may be possible to install a grid with conductive elements, pH sensors and acoustic sensors. For cases where the vaults or tanks cannot be entered prior to grout placement, a gridded system could be developed by placing the sensors on grids or poles (one dimensional grids) that can be lowered into the tanks, such as that shown in Figure 18. An advantage of this approach is that sensors could also be used to monitor the properties of the fresh system.

10 CONCLUSION

The long-term performance of a waste vault or a grout monolith will depend upon the chemical state of the monolith and the transport properties of both the vault and the monolith. The most important chemical property of the grout is the oxidation state; if the grout is oxidized sufficiently, it can release certain radionuclides. Therefore, the transport of oxygen into the grout, either via gas diffusion or as dissolved oxygen in permeating ground water, is a critical factor in long-term performance.

The gas diffusion and the hydraulic conductivity are the two primary transport coefficients for both the vault and the grout monolith. If both the vault and the grout remain intact throughout the desired period of performance, one could use existing transport/reaction models to predict the extent of oxidation. Cracks, however, can change transport coefficients dramatically. Moreover, the magnitude of the effect can depend upon the type of crack: parallel straight cracks, randomly distributed cracks, etc. In the absence of reliable models for predicting the initiation of cracking, monitoring provides a useful means of identifying changes in the structure before the detection of the release of radionuclides.

A number of techniques for monitoring the chemical and physical (cracking) state of the system have been summarized. A common disadvantage of current chemical state sensors is their limited lifetime, which restricts their utility as an embedded sensor; few have been demonstrated to operate in service, without maintenance, for more than a year. The physical sensors for crack initiation and crack extent are more promising. These sensors are typically metallic probes having a simple geometry, and the high pH of the materials should be compatible with these materials. Moreover, these types of probes are already being used in concrete construction.

An advantage of physical sensors over chemical sensors is that changes detected by the physical sensors will occur sooner than changes detected in the chemical sensors; sudden changes in the moisture content, oxygen content, or the reduction-oxidation potential would only occur after sudden changes in the transport coefficients. Therefore, a successful monitoring strategy could rely on linking validated physical sensors to reliable transport and reaction models to predict the current state of the facility.

11 REFERENCES

ACI (1990), “Control of Cracking in Concrete Structures,” ACI 224-90R, American Concrete Institute, Farmington Hills, MI.

ACI (1997), “Considerations for Design of Concrete Structures Subjected to Fatigue Loading,” ACI 215R-74 (92) (Reapproved 1997), American Concrete Institute, Farmington Hills, MI.

ACI (2007), “Report on Thermal and Volume Change Effects on Cracking of Mass Concrete, ACI 207R-07, American Concrete Institute, Farmington Hills, MI.

ACI (2011), “Building Code Requirements for Structural Concrete and Commentary,” ACI 318-11, American Concrete Institute, Farmington Hills, MI.

ACI (2012), “Report on Nondestructive Test Methods for Evaluation of Concrete In Structures,” ACI 228.2R-12, American Concrete Institute, Farmington Hills, MI.

Alden, A.S. and Munster, C.L. (1997), “Field Test of the In Situ Permeable Ground Water Flow Sensor,” *Ground Water Monitoring & Remediation*, Vol. 17, 81-88.

Angus, J.J. and Glasser, F.P. (1986), “The chemical environment in cement matrices,” Materials Research Society Symposium Proceedings, Number 50, p. 547.

ASTM (2009a), “Standard Test Method for Determining Age at Cracking and Induced Tensile Stress Characteristics of Mortar and Concrete under Restrained Shrinkage,” ASTM C1581/C1581M-09a, ASTM International, West Conshohocken, PA.

ASTM (2009b), “Standard Test Method for Autogenous Strain of Cement Paste and Mortar,” ASTM C1698-09, ASTM International, West Conshohocken, PA.

ASTM (2013), “Standard Test Method for Evaluating Plastic Shrinkage Cracking of Restrained Fiber Reinforced Concrete (Using a Steel Form Insert),” ASTM C1579-13, ASTM International, West Conshohocken, PA.

Attiogbe, E.K., Weiss, W.J., and See, H.T. (2004), “A Look At The Rate of Stress Versus Time of Cracking Relationship Observed In The Restrained Ring Test,” in *Advances in Concrete Through Science and Engineering*, Northwestern University, Evanston, IL, March 22-24, 2004 (on CD)

Bažant, Z.P. (1976), “Instability, ductility, and size effect in strain-softening concrete,” *Journal of the Engineering Mechanics Division* (ASCE), Vol. 102, pp. 331-344.

Bažant, Z. P., and Najjar, L. J. (1972), “Nonlinear water diffusion in nonsaturated concrete,” *Materials and Structures*, Vol. 5, pp. 3-20.

Bažant, Z. P., and Planas, J. (1998), *Fracture and Size Effect in Concrete and Other Quasi-Brittle Materials*, CRC Press, Boca Raton.

Bentur, A., Diamond, S., and Berke, N. (1997), *Steel Corrosion in Concrete*, Chapman & Hall, London.

Bernard, O. and Brühwiler, E. (2003), “The effect of reinforcement in the new layer on hygral cracking in hybrid structural elements,” *Materials and Structures*, Vol. 36, pp. 118-126.

Bishop, J.A., Pommerenke, D.J., Chen,G. (2011), “A rapid-acquisition electrical time-domain reflectometer for dynamic structure analysis,” *IEEE Transactions on Instrumentation and Measurement,* Vol. 60, 655-661.

Bontea, D.M., Chung, D.D.L. and Lee, G.C. (2000), "Damage in carbon fiber-reinforced concrete, monitored by electrical resistance measurement," *Cement and Concrete Research*, Vol. 30(4), pp. 651-659

Cao, J.Y. and Chung, D.D.L. (2001), "Defect dynamics and damage of concrete under repeated compression, studied by electrical resistance measurement," *Cement and Concrete Research*, Vol. 31(11), pp. 1639-1642.

Chen, P.W. and Chung, D.D.L. (1993), "Carbon-fiber-reinforced concrete for smart structures capable of nondestructive flaw detection," *Smart Materials*, Vol. 1916, pp. 445-453.

Chen, P.W. and Chung, D.D.L. (1995), "Carbon-fiber-reinforced concrete as an intrinsically smart concrete for damage assessment during dynamic loading," *Journal of the American Ceramic Society*, Vol. 78(3), pp. 816-818.

Chen, P.W. and Chung, D.D.L. (1996, "Concrete as a new strain stress sensor," *Composites Part B-Engineering*, Vol. 27(1), pp. 11-23

Dixon, K., Harbour, J., and Phifer, M. (November 2008), "Hydraulic and physical properties of saltstone grouts and vault concretes." Savannah River National Laboratory, SRNL-STI-2008-00421.

Egorov, O. B., Fiskum, S. K., O'Hara, M. J., Grate, J. W. (1999), "Radionuclide Sensors Based on Chemically Selective Scintillating Microspheres: Renewable Column Sensor for Analysis of ^{99}Tc in Water," *Analytical Chemistry*, Vol. 71, pp. 5420-5429.

Fagerlund, G. (1977), "The International Cooperative Test of the Critical Degree of Saturation Method of Assessing the Freeze/Thaw Resistance of Concrete," *Materials and Structures*, Vol. 10, No. 58, pp. 231-253.

Farrar, C.R. and Lieven, N.A.J. (2007), "Damage prognosis: the future of structural health monitoring," *Philosophical Transactions of the Royal Society a-Mathematical Physical and Engineering Sciences*, Vol. 365(1851), pp. 623-632.

Farrar, C.R. and Worden, K. (2007a), "An introduction to structural health monitoring," *Philosophical Transactions of the Royal Society a-Mathematical Physical and Engineering Sciences*, Vol 365(1851), pp. 303-315

Farrar, C.R. and Worden, K. (2007b), "Structural health monitoring – Preface," *Philosophical Transactions of the Royal Society a-Mathematical Physical and Engineering Sciences*, Vol. 365(1851), pp. 299-301.

FHWA (1997), "Guide to Nondestructive Testing of Concrete," FHWA-SA-97-105 (G.I. Crawford), Federal Highway Administration, Washington, DC.

Gilliam, T.M.; Spence, R.D.; Evans-Brown, B.S.; Morgan, I.L.; Shoemaker, J.L.; Bostick, W.D. (1988), "Performance testing of blast furnace slag for immobilization of technetium in grout," CONF-880903-18, Oak Ridge National Lab, Oak Ridge, TN.

Gilliam, T.M., Spence, R.D., Bostick, W.D., and Shoemaker, J.L. (1990), "Solidification/Stabilization of technetium in cement-based grouts," CONF-900256, Oak Ridge National Laboratory, Oak Ridge, TN; *Journal of Hazardous Materials*, Vol 24, pp. 189-197 (1990).

Goto, Y. (1971), "Cracks Formed in Concrete Around Deformed Tension Bars," *Proceedings of the American Concrete Institute*, Vol. 68, No. 4, pp. 244-251.

Grate, J.W., Egorov, O.B., O'Hara, M.J., and DeVol, T.A. (2008), "Radionuclide Sensors for Environmental Monitoring: From Flow Injection Solid-Phase Absorptiometry to Equilibration-Based Preconcentrating Minicolumn Sensors with Radiometric Detection," *Chem. Rev.*, Vol. 108, pp. 543-562.

Greenspan, L. (1977), “Humidity fixed points of binary saturated aqueous solutions,” *Journal of Research of the National Bureau of Standards*, Vol. 81A, pp. 89-96.

Gu, P., Xie, P. and Beaudoin, J.J., 1993a. Impedance characterization of microcracking behavior in fiber-reinforced cement composites. Cement and Concrete Composites, 15(3): 173-180.

Gu, P., Xu, Z.Z., Xie, P. and Beaudoin, J.J., 1993b. An AC impedance spectroscopy study of microcracking in cement-based composites during compressive loading. Cement and Concrete Research, Vol. 23(3), pp. 675-682.

Heimbuch, A. M., Gee, H. Y., DeHaan, A. J., and Leventhall, L. (1965), *Radioisotope Sample Measurement Techniques in Medicine and Biology;* International Atomic Energy Agency Symposium, Vienna, May 24-28; IAEA SM 61/65.

Hillerborg, A., Modwer, M., and Peterson, P. E. (1976), “Analysis of Crack Formation and Crack Growth in Concrete by Means of Fracture Mechanics and Finite Elements,” *Cement and Concrete Research*, Vol. 6, pp. 773-782.

Hixson, A.D., Woo, L.Y., Campo, M.A., Mason, T.O. and Garboczi, E.J. (2001), “Intrinsic conductivity of short conductive fibers in composites by impedance spectroscopy,” *Journal of Electroceramics*, Vol. 7(3), pp. 189-195.

Hsu, T.T.C, Slate, F. O., Struman, G. M., and Winter, G. (1963), "Microcracking of Plain Concrete and the Shape of the Stress Strain Curve", *Journal of the American Concrete Institute*, Vol. 60, pp. 209-224.

Hou, T.C. and Lynch, J.P. (2009), “Electrical impedance tomographic methods for sensing strain fields and crack damage in cementitious structures,” *Journal of Intelligent Material Systems and Structures*, Vol. 20(11), pp. 1363-1379.

Hung, K., (2007) “Application of Laser Shearography for Detecting Microcracks in Concrete,” MS Thesis, University of Maryland.

IAEA (2001), “Monitoring of Geological Repositories for High Level Radioactive Waste,” IAEA-TECDOC-1208, International Atomic Energy Agency, Vienna (Austria).

IAEA (2002), “Guidebook on non-destructive testing of concrete structures,” IAEA-TCS-17 (ISSN 1018–5518), International Atomic Energy Agency, Vienna (Austria).

IAEA (2005), “Non-destructive testing for plant life assessment,” IAEA-TCS-26 (ISSN 1018–5518), International Atomic Energy Agency, Vienna (Austria).

IAEA (2007), “Implementation Strategies and Tools for Condition Based Maintenance at Nuclear Power Plants,” IAEA-TECDOC-1551, International Atomic Energy Agency, Vienna (Austria).

Jansen, D.C., and Shah, S.P., (1997), “Effect of length on compressive strain softening of concrete,” *Journal of Engineering Mechanics*, Vol. 123, No.1, pp 25-35.

Kaplan, D.I. (2003), “Estimated Duration of the Subsurface Reducing Environment Produced by the Z-Area Saltstone Disposal Facility,” WSRC-RP-2003-00362 (Revision 0), Westinghouse Savannah River Company LLC, Aiken, SC 29808.

Khong, H., Amde, A.M., Ceesay, J., Livingston, R.A., Newman, J.W. (2007), “Application of laser shearography for detecting microcracks in concrete,” in *Proceedings of the First International Conference on Recent Advances in Concrete Technology*, A.M. Amde, G. Sabnis, and J.S.Y. Tan (Eds), Destech Publications, Lancaster, PA, pp. 175-184.

Kwak, H.-G., Ha, S.-J., and Weiss, W. J. (2010), "Experimental and Numerical Quantification of Plastic Settlement in Cementitious Systems," *Journal of Materials in Civil Engineering*, Vol. 22, pp. 951-966.

Laflamme, S., Kollosche, M., Connor, J.J., and Kofod, G. (2012), "Soft capacitive sensor for structural health monitoring of large-scale systems," *Structural Control & Health Monitoring*, Vol. 19, pp. 70-81.

Langmuir, D. (1997), *Aqueous Environmental Geochemistry*, Prentice-Hall, Inc., New Jersey.

Langton, C. and Weiss, W. J. (2012) "Transport Through Cracked Concrete: Literature Review," SRNL-STI-2012-00267, Savannah River National Laboratory 81 pp.

Lataste, J.F., C. Sirieix, D. Breysse, and M. Frappa, (2003), Electrical resistivity measurement applied to cracking assessment on reinforced concrete structures in civil engineering, NDT and E International, Vol. 36 pp. 383-394.

Laurent, S (2008), "Analysis of Groundwater from Taavinunannen," Report R-08-12, IVL, Swedish Environmental Research Institute, Stockholm.

Li, W., Pour-Ghaz, M., Castro, J., and Weiss, W. J. (2012), "Water Absorption and the Critical Degree of Saturation as it relates to Freeze-Thaw Damage in Concrete Pavement Joints," *Journal of Materials in Civil Engineering*, Vol. 24, pp. 299-307.

Lura, P., Pease, B., Mazzotta, G., Rajabipour, F., and Weiss, W. J. (2007), "Influence of Shrinkage-Reducing Admixtures on Evaporation, Settlement, and Plastic Shrinkage Cracking," *ACI Materials Journal*, Vol. 104, No. 2, pp. 187-194.

Macdonald, J.R. and William, R.K., 1987. Impedance spectroscopy: emphasizing solid materials and systems. Wiley-Interscience, New York

Mason, T.O., Campo, M.A., Hixson, A.D. and Woo, L.Y. (2002), "Impedance spectroscopy of fiber-reinforced cement composites," *Cement & Concrete Composites*, Vol. 24(5), pp. 457-465.

McCreery, R.L. (1999), in *Electrochemical Properties of Carbon Surfaces, Interfacial Chemistry* (A. Wiechowski, Editor), Chapter 35, pp. 631-647, Dekker, New York.

Mindess, S., Young, J.F., and Darwin, D. (2002), *Concrete*, 2nd Edition, Prentice Hall.

Mollo, L. and Greco, R. (2011) "Moisture Measurements in Masonry Materials by Time Domain Reflectometry," *Journal of Materials in Civil Engineering*, Vol. 23, pp. 441-444.

Naus, D.J. (2009), "Inspection of Nuclear Power Plant Structures – Overview of Methods and Related Applications," ORNL/TM-2007/191, Oak Ridge National Laboratory, Oak Ridge, TN.

Naus, D.J. and Graves, H.L. (2000), "Detection of Aging of Nuclear Power Plant Structures," in *OECD-NEA Workshop on the Instrumentation and Monitoring of Concrete Structures*, NEA-CSNI-R(2000)15, Brussels, Belgium, pp. 19-58.

Niemuth, M. (2004), "Using impedance spectroscopy to detect flaws in concrete," Masters Thesis, Purdue University, West Lafayette, IN.

Nordstrom, D.K. and Wilde, F.D. (2005), "Reduction-Oxidation Potential (Electrode Method)," in *U.S. Geological Survey Techniques of Water-Resources Investigations* (Chapter 6.5) (http://water.usgs.gov/owq/FieldManual)

Pabalan, R. T., Glasser, F. P, Picket, D. A., Walter, G. R., Biswas, S., Juckett, M.R., Sabido, L. M., and Myers, J. L. (2009), "Review of Literature and Assessment of Factors Relevant to Performance of Grouted Systems of Radioactive Waste Disposal," US Nuclear Regulatory Commission, NRC 02-07-006.

Page, C.L. and Lambert, P. (1987), “Kinetics of oxygen diffusion in hardened cement pastes,” *Journal of Materials Science*, Vol. 22, pp. 942-946.

Pease, B. J., Geiker, M., Stang, H., and Weiss, W. J. (2010), “The design of an instrumented rebar for assessment of corrosion in cracked reinforced concrete,” *Materials and Structures*, Vol. 44, pp. 1259-1271.

Peled, A., Torrents, J.M., Mason, T.O., Shah, S.P. and Garboczi, E.J. (2001), “Electrical impedance spectra to monitor damage during tensile loading of cement composites,” *ACI Materials Journal*, Vol. 98(4), pp. 313-322.

Popovics, S., Rose, J.l., and Popovics, J., S., (1990), “The behavior of ultrasonic pulses in concrete,” Cement and Concrete Research, Vol 20, No. 2, pp. 259-270

Pour-Ghaz, M., Kim, J., Nadukuru, S.S., O’Connor, S., Michalowski, R.L., Bradshaw, A., Green, R.A., Lynch, J.P., Poursaee, A., Weiss, J. (2011), “Using electrical, magnetic and acoustic sensors to detect damage in segmental concrete pipes subjected to permanent ground displacement,” *Cement and Concrete Composites*, Vol. 33(7), pp. 749-762.

Pour-Ghaz, M., Spragg, R., Weiss, J. (2012) “Can Acoustic Emission be used to Detect Alkali Silica Reaction Earlier than Length Change?” in *14th International Conference on Alkali-Aggregate Reaction*, 2012, University of Texas, Austin

Pour-Ghaz, M., Poursaee, A., Spragg, R., Weiss, W. J. (2011) “Experimental Methods to Detect and Quantify Damage in Restrained Ring Specimens,” *Journal of Advanced Concrete Technology*, Vol. 9(3), pp. 251-260.

Pour-Ghaz, M. and Weiss, J. (2010a), “Detecting the time and location of cracks using electrically conductive surfaces,” *Cement and Concrete Composites*, Vol. 33(1), pp. 119-123.

Pour-Ghaz, M. and Weiss, J. (2010b), “Quantifying damage due to aggregate expansion in cement matrix,” In: *Advances in the Material Science of Concrete*, J. H. Ideker and A. Radlinska (Editors), ACI SP-270, American Concrete Institiute.

Pour Ghaz, M., and Weiss, W. J., (2011) “Application of Frequency Selective Circuits for Crack Detection in Concrete Elements,” *Journal of ASTM International*, Vol. 8(10), Paper ID JAI103826 (available online).

Poursaee, A., and Weiss, W. J. (2010), “An Automated Electrical Monitoring System (AEMS) to Assess Concrete Property Development,” *Journal of Automation in Construction*, Vol. 19, Issue 4, pp. 485-490

Puri, S., and Weiss, W. J. (2003), “Assessing Damage Localization In Concrete Cylinders Tested In Compression,” The Seventh International Symposium On Brittle Matrix Composite, 13-15 October 2003, Editors A Brandt, V. Li, and Marshall, BMC 07, Woodhead Publishers, pp. 111-120.

Puri, S., and Weiss, W. J. (2006), “Assessment of Localized Damage in Concrete under Compression Using Acoustic Emission,” *Journal of Materials in Civil Engineering*, Vol. 18, pp. 325-333.

Qi, C., W. J. Weiss, W.J., and J. Olek, J. (2003), “Characterization of Plastic Shrinkage Cracking in Fiber-Reinforced Concrete Using Semi-Automated Image Analysis,” *Concrete Science and Engineering*, Vol. 36, No. 260, pp. 386–395.

Raoufi, K., and Weiss, W. J. (2012), “Using internal curing to mitigate early-age cracking and increase the performance of reinforced concrete with respect to corrosion”, ACI Presentation Publications, (http://www.concrete.org/Convention/fall-Convention/PresenterHandouts.asp?SessionID=00004179&CurrentDay=10%2F23%2F2012).

Reza, F., Batson, G.B., Yamamuro, J.A. and Lee, J.S., 2003. Resistance changes during compression of carbon fiber cement composites. *Journal of Materials in Civil Engineering*, Vol. 15, pp. 476-483.

RILEM (1999), "Environmental design method in materials and structural engineering - Progress Report of RILEM TC 172-EDM/CIB TG 22," *Materials and Structures*, Vol. 32, Issue 224, pp. 699-707.

RILEM (2003), *Early Age Cracking in Cementitious Systems*, A. Bentur Ed., 350 pp., RILEM, Bagneux, France, 350 pp.

Ritz, G.F. and Collins, J.A. (2008), "pH" in *U.S. Geological Survey Techniques of Water-Resources Investigations* (Chapter 6.4) (http://water.usgs.gov/owq/FieldManual)

Sant, G., Lura, P., and Weiss, W. J. (2006) "Measurement of Volume Change in Cementitious Materials at Early Ages: Review of Testing Protocols and Interpretation of Results," *Transportation Research Record*, Vol. 1979, pp. 21-29, doi 10.3141/1979-05,

Schüring, J., Schulz, H.D., Fischer, W.R., Böttcher, J., and Duijnisveld, W.H.M. (1999) *Redox: Fundamentals, Processes, and Applications*, Springer-Verlag, Berlin.

Scott, I.G. (1991), *Basic Acoustic Emission*, part of *Nondestructive Testing Monographs and Tracts – Vol. 6*, Gordon and Breach Science Publishers, New York.

Seppanen, A., K. Karhunen, A. Lehikoinen, and J.P. Kaipio, and P.Monteiro, (2009), Electrical resistance tomography imaging of concrete, Concrete Repair, Rehabilitation, and Retrofitting II, Alexander et al, (eds), pp 571-577, Taylor and Francis Group, London.

Shah, S. P. and Slate, F.O. (1965), "Internal Micro-Cracking, Mortar-Aggregate Bond, and Stress Strain Curve of Concrete," Proc. International Conference on the Structure of Concrete, Imperial College, London, England, pp. 1–11.

Shah, S. P., Swartz, S. E., and Ouyang, C. (1995), *Fracture Mechanics of Concrete*, John Wiley & Sons.

Srinivasan, R., Phillips, T.E., Bargeron, C.B., Carlson, M.A., Schemm, E.R., and Saffarian, H.M. (2000), "Embedded micro-sensor for monitoring pH in concrete structures," in *Smart Structures and Materials 2000: Smart Systems for Bridges, Structures, and Highways*, S.C. Liu (Editor), (*Proceedings of the SPIE Vol. 3988*), 40-44.

Stark, D.C. (1980), "Alkali-Silica Reactivity: Some recommendations", *Cement, Concrete, and Aggregates*, Vol. 2, No. 2, pp. 92-94.

Stumm, W. and Morgan, J.J. (1981), *Aquatic Chemistry*, (Second Edition), John Wiley & Sons, New York.

Suaris, W., and Fernando, V., (1987) "Ultrasonic Pulse Attenuation as a Measure of Damage Growth During Cyclic Loading of Concrete," *ACI Materials Journal*, Vol. 84, No. 3, pp. 185-193.

Švancara, I, Walcarius, A, Kalcher, K., and Vytřas, K. (2009), "Carbon paste electrodes in the new millennium," *Central European Journal of Chemistry*, Vol. 7, pp. 598-656.

Taylor, H.F.W. (1990), *Cement Chemistry*, Academic Press, New York.

Topp, G.C., Davis, J.L., and Annan, A.P. (1980), "Electromagnetic determination of soil water content: Measurements in coaxial transmission lines," *Water Resources Research*, Vol. 16, pp. 574-582.

Torrents, J.M., Mason, T.O. and Garboczi, E.J. (2000), "Impedance spectra of fiber-reinforced cement-based composites - A modeling approach," *Cement and Concrete Research*, Vol. 30(4), pp. 585-592.

Torrents, J.M., Easley, T.C., Faber, K.T., Mason, T.O. and Shah, S.P. (2001a), “Evolution of impedance spectra during debonding and pullout of single steel fibers from cement,” *Journal of the American Ceramic Society*, Vol. 84(4), pp. 740-746.

Torrents, J.M., Mason, T.O., Peled, A., Shah, S.P. and Garboczi, E.J. (2001b), “Analysis of the impedance spectra of short conductive fiber-reinforced composites,” *Journal of Materials Science*, Vol. 36(16), pp. 4003-4012

TRB (2006), “Control of Cracking in Concrete: State of the Art,” TRB Circular E-C107, Transportation Research Board, Washington, D.C.

Uhlig, H.H. and Revie, R.W. (1985), *Corrosion and Corrosion Control*, Wiley-Interscience, New York.

Van Mier. (1999), “Towards an Universal Theory for Fracture of Concrete,” in *Mechanics of Quasi-Brittle Materials and Structures*, G. Pijaudier-Cabot, Z.Bittnar and B. Gerard (eds.), HERMES Science Publication, Paris, pp. 17 – 30.

Weiss, W.J., (1999) “Prediction of early-age shrinkage cracking in concrete”, Northwestern University, Evanston

Weiss, W. J., Yang, W., and Shah, S. P. (1998), "Shrinkage Cracking of Restrained Concrete Slabs.” *Journal of Engineering Mechanics Division* (ASCE), Vol. 124, No. 7, pp. 765-774.

Weiss, W. J., Shane, J. D., Mieses, A., Mason, T. O., and Shah, S. P., (1999) “Assessing the Moisture Migration in High Strength Concrete Using Impedance Spectroscopy.” Second Symposium on the Importance of Self Desiccation in Concrete Technology, Lund Sweden, pp. 31-48

Weiss, J., Olek, J. and Nantung (2000), “Interaction Between Micro-Cracking, Cracking and Reduced Durability in Concrete: Developing Methods for Considering Cumulative Damage in Life-Cycle Modeling,” INDOT JTRP Project Proposal.

Weiss J., and Olek, J., (2005) “An overview of recent applications of acoustic emission to the study of damage development in portland cement concrete materials,” Proceedings of the XXII Conference on Structural Failures, Szczecin-Miedzyzdroje, Poland, May 17-20, 2005, pp. 70-83

Weiss W. J., Radlinska A., Paradis F., Niemuth M., and Sant G. (2007), ‘Cracks in Concrete: an Overview of an Approach to Assess Their Development, Their Physical Features, and Their Impact on Durability’, RILEM Workshop: Transport Mechanisms In Cracked Concrete, Ghent (2007).

Whitfield, M.S. (1974), “Thermodynamic limitations on the use of the platinum electrode in Eh measurements,” *Limnology and Oceanography*, Vol. 19, pp. 857-865.

Wikberg, P. (1985), “The assessment of reducing conditions at depth in granitic rock,” in *Scientific Basis for Nuclear Waste Management IX*, *Mat. Res. Soc. Symp. Proc.*, Vol. 50, (Lars O. Werme, Ed.) pp. 137-144, Materials Research Society.

Wittmann, F.H. (2009), “Heresies on shrinkage and creep mechanisms,” in *Creep, Shrinkage and Durability Mechanics of Concrete and Concrete Structures*, Tanabe et al. (Eds.), Taylor & Francis Group, London (ISBN 978-0-415-48508-1), pp. 3-9.

Yang , Z., Weiss, J., and Olek, J. (2006), “Water Transport in Concrete Damaged by Tensile Loading and Freeze-Thaw Cycling,” *Journal of Materials in Civil Engineering*, Vol. 18(3), pp. 424-434.

Yoon, S., Wang, K., Weiss, W. J., and Shah, S. P. (2000a), “The Interaction between Loading, Corrosion, and Serviceability of Reinforced Concrete,” *ACI Materials Journal*, Vol. 97, no. 6, pp. 637-644.

Yoon, D. J., Weiss, W. J., and Shah, S. P. (2000b), “Detecting the Extent of Corrosion with Acoustic Emission,” Transportation Research Record 1698, pp. 54-60.

Young, M.H., Warrick, A.W., Wierenga, P.J, Hofmann, L.L., and Musil, S.A. (1999), “Comparing Monitoring Strategies at the Maricopa Environmental Monitoring Site, Arizona,” NUREG/CR-5698, U.S. Nuclear Regulatory Commission.

NRC FORM 335
(12-2010)
NRCMD 3.7

U.S. NUCLEAR REGULATORY COMMISSION

BIBLIOGRAPHIC DATA SHEET

(See instructions on the reverse)

1. REPORT NUMBER
(Assigned by NRC, Add Vol., Supp., Rev., and Addendum Numbers, if any.)

NUREG/CR-7169

2. TITLE AND SUBTITLE

Sensors and Monitoring to Assess Grout and Vault Behavior for Performance Assessment

3. DATE REPORT PUBLISHED

MONTH	YEAR
June	2014

4. FIN OR GRANT NUMBER

V6281

5. AUTHOR(S)

Kenneth A. Snyder and W. Jason Weiss

6. TYPE OF REPORT

Technical

7. PERIOD COVERED (Inclusive Dates)

8. PERFORMING ORGANIZATION - NAME AND ADDRESS (If NRC, provide Division, Office or Region, U. S. Nuclear Regulatory Commission, and mailing address; if contractor, provide name and mailing address.)

National Institute of Standards and Technology

9. SPONSORING ORGANIZATION - NAME AND ADDRESS (If NRC, type "Same as above", if contractor, provide NRC Division, Office or Region, U. S. Nuclear Regulatory Commission, and mailing address.)

Division of Risk Assessment, Office of Nuclear Regulatory Research, US Nuclear Regulatory Commission

10. SUPPLEMENTARY NOTES

11. ABSTRACT (200 words or less)

To support performance assessment (PA) of waste vaults and grout monoliths, the National Institute of Standards and Technology (NIST) has performed a preliminary evaluation of the state-of-the-art of sensors, nondestructive evaluation methods, and any relevant geophysical techniques that may be used to quantify changes to the intended chemical (e.g. redox state) and structural properties (e.g. crack initiation, development and propagation) of large engineered waste isolation systems. If the vaults and monoliths remain intact, the system performance should be consistent with the successful performance anticipated from the PA. Events such as cracking, however, could lead to significant changes in the overall vault or monolith performance. Measurement techniques that could be used to detect the onset of cracks and to detect changes in the chemical are summarized in the context of a monitoring program.

12. KEY WORDS/DESCRIPTORS (List words or phrases that will assist researchers in locating the report.)

cement, grout, saltstone, cracks, monitoring, crack sensors, structural health monitoring, acoustic emissions, crack monitoring, geophysics

13. AVAILABILITY STATEMENT

unlimited

14. SECURITY CLASSIFICATION

(This Page)

unclassified

(This Report)

unclassified

15. NUMBER OF PAGES

16. PRICE

Printed
on recycled
paper

Federal Recycling Program

UNITED STATES
NUCLEAR REGULATORY COMMISSION
WASHINGTON, DC 20555-0001

OFFICIAL BUSINESS

NUREG/CR-7169

Sensors and Monitoring to Assess Grout and Vault Behavior for Performance Assessments

June 2014